Journal of Medicinal Chemistry

Article

Preparation, antiepileptic activity and cardiovascular safety of dihydropyrazoles as brain-penetrant T-type calcium channel blockers

Lubos Remen, Olivier Bezençon, Lloyd Simons, Rick D. Gaston, Dennis Downing, John Gatfield, Catherine Roch, Melanie Kessler, Johannes Mosbacher, Thomas Pfeifer, Corinna Grisostomi, Markus Rey, Eric A. Ertel, and Richard Moon

J. Med. Chem., **Just Accepted Manuscript** • DOI: 10.1021/acs.jmedchem.6b00756 • Publication Date (Web): 31 Aug 2016

Just Accepted

ACS Publications

Journal of Medicinal Chemistry is published by the American Chemical Society. 1155 Sixteenth Street N.W., Washington, DC 20036

Preparation, antiepileptic activity and cardiovascular safety of dihydropyrazoles as brain-penetrant T-type calcium channel blockers

Lubos Remen[1], Olivier Bezençon[1], Lloyd Simons[2], Rick Gaston[2], Dennis Downing[2†], John Gatfield[1], Catherine Roch[1], Melanie Kessler[1], Johannes Mosbacher[1†], Thomas Pfeifer[1†], Corinna Grisostomi[1], Markus Rey,[1] Eric A. Ertel[1] and Richard Moon[1]*

[1]Drug Discovery Chemistry, Biology and Pharmacology, Actelion Pharmaceuticals Ltd., Gewerbestrasse 16, CH-4123 Allschwil, Switzerland

[2]Kalexsyn, Inc., 4502 Campus Drive, Kalamazoo, Michigan 49008, USA

ABSTRACT: A series of dihydropyrazole derivatives was developed as potent, selective, brain-penetrating T-type calcium channel blockers. An optimized derivative, compound **6c**, was advanced to *in vivo* studies, where it demonstrated efficacy in the WAG/Rij rat model of generalized non-convulsive, absence-like epilepsy. Compound **6c** was not efficacious in the basolateral amygdala kindling rat model of temporal lobe epilepsy, and it led to prolongation of the PR interval in ECG recordings in rodents.

INTRODUCTION

Epilepsy represents one of the most common chronic brain diseases. It is estimated that 0.5% to 1% of the worldwide population will experience at least one unprovoked seizure in their lifespan[1]. Epilepsy is a brain disorder characterized by an enduring predisposition to generate epileptic seizures and by the neurobiological, cognitive, psychological, and social consequences of this condition[2]. Epileptic patients experience recurrent spontaneous seizures, which may present various phenotypes ranging from mild brief lapses of attention or muscle jerks up to severe and prolonged convulsions. Seizures are transient events due to abnormal, excessive or synchronous neuronal activity in the brain. They are classified either as focal seizures when they remain restricted to networks in one hemisphere or as generalized seizures when they rapidly engage bilaterally distributed networks. Etiologies and clinical presentations are multiple, so that the so-called epileptic syndromes are classified in approximately sixty different types and sub-types based on features such as clinical observations, electroencephalographic (EEG) pattern, age of onset, cognitive and developmental antecedents and consequences, provoking or triggering factors, that also includes genetic variations.

Many antiepileptic drugs (AEDs) exert their actions through direct or indirect modulation of ion channels . Foremost pharmacological targets are $GABA_A$-receptors (targeted by diazepam and other benzodiazepines), voltage-gated sodium channels (targeted by carbamazepine[3], lacosamide[4], lamotrigine[5], zonisamide[6] and others), voltage-gated potassium channels (retigabine[7]), and high voltage-gated calcium channels (lamotrigine[8], levetiracetam[9], topiramate[10]). More recently an AMPA receptor blocker, perampanel, was approved as AED[11]. In spite of about 25 commercially-available AEDs, about one in three epileptic patients remains or develops pharmacoresistant, meaning that sustained seizure freedom is not achieved following

tryout of two tolerated and appropriately chosen and used AED schedules (whether as monotherapy or in combination)[12]. This proportion, which has not decreased markedly for more than a century[13], clearly calls for new compounds with new mechanisms of action. At Actelion Pharmaceuticals, we decided to target T-type calcium channels and to develop a new mechanism-based inhibitor that could be useful to treat epilepsy.

Low-voltage-gated T-type calcium channels (TTCCs) are the products of three different genes in mammals, CACNA1G, CACNA1H, and CACNA1I, leading to the $Ca_v3.1$, $Ca_v3.2$, and $Ca_v3.3$ channels, respectively[14]. They are largely expressed in the brain[15], particularly in the thalamus and cortex areas, suggesting an important role in thalamocortical signaling and rhythms. TTCCs play a critical role in idiopathic generalized epilepsies (IGE), such as absence epilepsy, both in humans and in animals[16]. Ethosuximide, the drug of choice for absence epilepsy[17], has been claimed to block TTCCs at pharmacologically relevant concentrations[18]. Genetic variants of the human CACNA1H gene have been linked to absence epilepsies[19] and those variants are predicted to increase neuronal excitability either by altering the biophysical properties of the channel or by increasing surface expression,[16d, 19a, 20] and thereby to influence neuronal excitability. In addition, $Ca_v3.1$-knock-down mice are more resistant to absence-type seizures than their wild type littermates[21]. More recently, TTCC antagonists were shown to attenuate or to suppress seizures in the WAG/Rij rat[22] and the GAERS rat[23], two genetic animal models for absence-like epilepsy[24]. Information on the efficacy of TTCC blockers in other types of epilepsies has remained sparse: a role for TTCCs has been suggested in temporal lobe epilepsy[25] but the effect of a selective TTCC blocker in relevant animal models has not been shown.

Brain penetrant, selective TTCC blockers have been reported only recently. As mentioned above, ethosuximide has been claimed to block TTCCs, and zonisamide also blocks TTCCs in

the micromolar range[6, 26]. A first selective TTCC blocker **1** (MK-8998, presumed structure, Figure 1, IC_{50}-values of 1.2 nM, 8.2 nM and 1.5 nM on the $Ca_v3.1$-, $Ca_v3.2$-, and $Ca_v3.3$-channels respectively, in our hands) was evaluated in phase 1 and phase 2 clinical trials, targeting acute psychosis in patients with schizophrenia[27]. Another compound **2** (Z-944, IC_{50}-values of 37 nM, 73 nM and 86 nM on the $Ca_v3.1$-, $Ca_v3.2$-, and $Ca_v3.3$-channels respectively, in our hands) was in phase 1 clinical trials and may have proceeded to phase 2 for neuropathic pain[28]. Several other potent, selective TTCC blockers have been used in preclinical research to investigate different indications, such as pain[29], essential tremor[30], Parkinson disease[31], obesity[32], addiction[33], or psychosis[34].

Our program started with the development of high-throughput FLIPR-assays using conditions similar to those published previously[35]. Since genetic variants of the CACNA1H gene had the strongest link to idiopathic generalized epilepsies[19], we selected $Ca_v3.2$ for the high-throughput screening (HTS) and we measured block of $Ca_v3.1$ and $Ca_v3.3$ in secondary assays. We developed a counter assay on $Ca_v1.2$, an L-type high voltage activated calcium channel, to assess the selectivity profile of our hits and to avoid major cardiovascular side-effects such as hypotension[36].

RESULTS AND DISCUSSION

From our HTS campaign, we identified dihydropyrazole **5a** (Table 1) as a compound with a promising potency on $Ca_v3.2$, and with good selectivity toward $Ca_v1.2$. A three step synthesis following known procedure[37] gave us a rapid access to this class of compounds, presented in Tables 1 and 2. An aldol condensation between a benzaldehyde and a methylphenyl ketone (Scheme 1) yielded α,β-unsaturated ketones of type **3**. Cyclization with hydrazine led to

dihydropyrazoles of type **4**, which were converted immediately to the final, desired (racemic) products of type **5** or **6**. Non-acylated dihydropyrazoles of type **4** proved to be unstable on storage, oxidizing rapidly to the corresponding pyrazoles. Slight modifications led to amide derivative **5i** and to thiourea **5m** (see supporting information for experimental details). This approach allowed a straightforward investigation of the structure activity relationship (SAR) at the urea moiety (Table 1). We found that an electron withdrawing, *para* fluoro substituent increased the potency on $Ca_v3.2$ (compound **5b**). A *meta* fluorine substituent did not contribute to potency (compound **5c**), while an *ortho* fluorine substituent (compound **5d**) was not tolerated. Electron donating or electron neutral substituents at position 4 were detrimental (compounds **5e** and **5f**). Replacing the phenyl substituent by a cycloalkyl or an alkyl group (compounds **5g** and **5h**) led to a decrease in potency and in selectivity versus $Ca_v1.2$. Replacing the urea either by an amide (compound **5i**), or by a thiourea (compound **5m**), or elongating the urea substituent (compound **5j**) led to lower potencies as well. Finally the presence of heteroaryls, like a pyridinyl in derivatives **5k** and **5l** was not tolerated.

This first SAR investigations led to potent $Ca_v3.2$ blockers (compounds **5b**, **5c**). On the other hand, these compounds contained four aromatic rings and a urea functionality and were therefore poorly soluble (< 1mg/L in aqueous buffer, see Table 5 for selected examples). The development of an SAR at the other two aryl positions proved more complex, since it required the introduction of diversity at the very first step of the synthesis. Therefore, we focused on substituents that might improve solubility. Complete removal of an aryl substituent at either position 3 or 5 led to a loss in potency (Table 2, compounds **6b** and **6e**) but suppression of the *para*-bromo substituent on Ar^1 was well tolerated (compound **6a**). To our delight, introduction of a 4-pyridinyl group at the Ar^1-position was tolerated (compound **6c**), while the corresponding *N*-oxide (compound **6d**)

was less potent. At the Ar^2-position, a *para*-methyl sulfone led to a potent blocker (compound **6f**) but a combination of polar substituents at both Ar^1- and Ar^2-positions was not tolerated well (compound **6g**). Selectivity toward $Ca_v1.2$ was well retained throughout the compound series.

We also attempted to increase solubility by introducing a new substituent bearing a polar, solubilizing group. One possibility was offered by the quaternization of the chiral center. This quaternization should not only allow us to introduce a hydrophilic substituent (*vide infra*) but it would prevent a possible aromatization, and it would increase the proportion of rotatable, non-aromatic bonds[38]. As outlined in Scheme 2[37b], acylation of an activated alkyne led to Michael acceptors of type **7**, that upon addition of an aryl cuprate yielded compounds of type **8** Cyclization with hydrazine (compounds of type **9**), formation of the urea (compounds of type **10**), and deprotection led to final products **11a-l**. We observed that at this position a hydroxymethyl substituent was well-tolerated (Table 3, compound **11a**) and an elongated, polar hydroxyethyl group was also tolerated (compound **11b**). Based on this last substituent, we found that the potentially solubilizing 4-methoxyethoxy substituent on Ar^2 (compound **11c**) led to a potent $Ca_v3.2$ blocker, in contrast to a tertiary amine (compound **11d**). Compound **11c** was indeed slightly soluble in aqueous buffer, and replacement of a phenyl by a 4-pyridinyl (compound **11e**) led to a moderate loss in potency but increased solubility from < 1mg/L to 35 mg/L in aqueous buffer at pH7 (Table 5). Further combinations of polar groups led to diverse results; while compound **11f** still retained most of its potency, and some solubility, compound **11g** proved to be less potent, most probably being too polar. Additional modifications at the polar chain, in particular introduction of tertiary amines, were not well tolerated (Table 4, compound **11i-11l**), even if these examples displayed a sufficient solubility profile (Table 5, compounds **11k** and **11l**). From the solubility profiles presented in Table 5, no simple trend can

be found between physicochemical properties and solubility, demonstrating the complexity of the factors controlling this parameter. In general, an ionizable substituent has to be introduced (compounds **6c**, **11e**, **11f**, **11k** and **11l**) but compound **11c** represent an exception. Unfortunately, gain in solubility often happened at the detriment of potency toward the target. Indeed, it seems that the high potency values observed on $Ca_v3.2$ in this series are at least partially driven by lipophilicity, even if a high polar surface area (PSA) is sometimes tolerated (compounds **6f**, **11c**, and **11f**). The most potent derivative, compound **5b**, has a PSA of 44.7 $Å^2$, and a very high clogP value of 5.5. In terms of ligand efficiency (LE), the best blockers described here are compounds **6a** (LE = 0.38), and **6c** (LE = 0.37), which can be regarded as reasonable values. The lipophilic ligand efficiencies (LLE), though, remain low. The best value is obtained for compound **6c** (LLE = 3.6), clearly inferior to the threshold value of 5 recommended in the literature[39].

Since our goal was to achieve brain penetration, we monitored the central nervous system multiparameter optimization (CNS-MPO)-values[40] as well. When considering compounds with a minimum of solubility, we realized that these values were rather low, in particular due to high clogP, clogD, and molecular weight. For instance MPO values for compounds **6f**, **11c**, and **11f**, were of 3.8, 2.8, and 3.2, respectively. Selected compounds were measured in a multi-drug resistance gene 1 (MDR1) assay with a transfected MDCK cell line to assess their brain permeability and their potential as P-glycoprotein (P-gp) substrates (Table 6). While compound **6c** was permeable and was not effluxed by P-gp, the more polar compounds **11f** and **11g** remain permeable but were clearly substrates for P-gp. A limit with a PSA around 60 $Å^2$ seemed to emerge. At this stage it became clear that the ridge between adequate solubility and problematic efflux substrate would be very narrow for this class of compounds, and we decided to use compound **6c**, which displayed acceptable solubility, as a model compound.

As mentioned earlier all blockers were, up to now, prepared and tested as racemates. At this stage, we prepared the reasonably potent compound **11h** (Table 3), a very close analogue to compound **11f**, we separated its enantiomers by HPLC using a chiral solid phase, and we crystallized one enantiomer to determine its absolute configuration by X-ray diffraction analysis. This enantiomer was (*S*)-configured (compound **(*S*)-11h**, Fig. 2) and this allowed us to identify the (*R*)-enantiomer as being the active one for compound **11h** (Table 3). By analogy, we assumed that the (*R*)-enantiomer was responsible for the observed biological activity in all compounds **11a-11g**, and that the (*S*)-enantiomer should be the active one for compounds **5a-5m** and **6a-6g**. Due to its importance, the enantiomers of compound **6c** were separated as well (Table 2). The discrimination between the enantiomers was not as marked in this case as for compounds **(*R*)-11** and **(*S*)-11**. Nevertheless, a factor ten difference in potency was observed on the cav3.2 channel.

Compound **6c** proved to be a rather well balanced blocker for all three channels $Ca_v3.1$, $Ca_v3.2$, and $Ca_v3.3$, with a somewhat lower affinity for $Ca_v3.3$ (Table 7). The Ca^{2+}-FLIPR assay used to characterize and optimize our blockers did not control cell membrane potential, which rests spontaneously at around -25 mV in these cells. Therefore, IC_{50}-values measured in this system mostly reflect compound binding to channels in the inactivated state[41]. In order to measure IC_{50}-values reflecting compound binding to channels in the closed or open states, we set up automated patch-clamp (QPatch) measurements using resting potentials at -90 mV and -60 mV. From these experiments, compound **6c** displayed a moderate voltage-dependence on all three TTCCs. Compound **6c** proved to be selective toward other channels: weak inhibition of $Ca_v1.2$ was observed (Table 2) as well as weak inhibition of endogenous voltage regulated sodium and potassium channels in rodent neurons (Table 7). Most probably owing to its basic

pyridinyl moiety, compound **6c** blocked the hERG channel with an IC_{50}-value of 0.8 μM. It should be noted that this was rather an exception within this series. For instance, both compound **5a** and compound **5c** blocked the hERG channel with IC_{50}-values above 10 μM. On the other hand, compound **6c** inhibited CYP3A4, due to its 4-pyridinyl moiety. The CYP2C9 was inhibited as well, on the contrary to CYP2D6. It was metabolically rather stable using human, rat and mouse microsomes, it had an unbound fraction of 2-3% in rat and human plasma (Table 7) and a good permeability (Table 6): these data encouraged us to profile this compound in vivo.

A first pharmacokinetic (PK) study in rats (Table 8) indicated a systemic clearance equal to liver blood flow, in spite of its low intrinsic clearance in rat microsomes (Table 7, 104 μL/min.mg protein, or about 10 mL/min·kg, with $f_{u,microsomes} = 0.5$) and in rat hepatocytes ($Cl_{intr.}$ = 5.7 μL/min·10^6 cells). The high *in vivo* clearance led to low exposure after oral administration at a dose of 2 mg/kg. However, oral co-administration of the general broad-band CYP-inhibitor aminobenzotriazol (ABT) 2 hours before application of the iv dose led to an almost complete suppression of clearance, indicating that oxidative clearance by the CYP-enzymes represented the main metabolism pathway for this compound in rats. Under this condition, the compound was quantitatively bioavailable, confirming excellent absorption properties. In dogs (without ABT), an acceptable maximal concentration was observed after oral dose of 10 mg/kg. Brain exposure was studied as well, albeit with higher doses, in order to saturate metabolism and achieve pharmacologically relevant concentrations (Table 9). Indeed, plasma concentrations at 1 and 3 h post-dose indicated a non-linear behavior between 2 and 10 mg/kg (compare data in Tables 8 and 9), most probably due to a saturation of metabolism at the higher dose. The compound penetrated the brain very well at all doses between 10 and 100 mg/kg and the CSF concentrations were in a fair agreement with the unbound concentrations in plasma.

Since there is a strong rationale for a role of TTCCs in idiopathic generalized epilepsies including absence epilepsy, we tested the efficacy of compound **6c** in the WAG/Rij rat (Wistar albino rats of Glaxo Rijswijk) model of generalized non-convulsive absence-like epilepsy. Male WAG/Rij rats older than 6 months were implanted with radiotelemetry probes allowing continuous recording of the electroencephalogram/electromyogram and they were administered with a single oral dose of 100 mg/kg compound **6c** (or matching vehicle) at the beginning of their nocturnal active phase. Compound **6c** decreased by 63.5 % the number of seizures over the 12 h night period compared to vehicle ($p = 0.0013$, paired t-test; Fig. 3A), corresponding to a decrease of 62.2 % of the total duration of the seizures during this period (or 1239 seconds; Fig. 3B). Over the first 4 h following administration, spontaneous seizures were nearly completely suppressed by compound **6c** with a decrease of more than 99 % of the number and duration of seizures compared to vehicle. From the brain exposure experiment (Table 9), at 1 h $C_{u,brain}$ is equal to 128 nM. This is above the IC_{50}-values for the $Ca_v3.1$- and $Ca_v3.2$ channels in our FLIPR assay, while the other IC_{50}-values are above this concentration. We can hypothesize that either the Cav3.3 channel is less important for the generation of seizure in this animal model, or that the IC_{50}-values do not need to be reached to already have a full suppression of seizures. Further, a compound blocking the channels at the inactivated state seems to be sufficient to prevent seizures. Those data are in accordance with published studies showing strong reductions of seizures in this model with potent TTCC blockers[22, 42].

We also tested compound **6c** at 300 mg/kg p.o. in the basolateral amygdala kindling rat model of temporal lobe epilepsy (a type of focal epilepsies). In this model, animals are electrically stimulated daily in the basolateral amygdala until they are fully kindled, i.e. until they reach robust occurrence of stage 5 seizures on Racine's scale at each stimulation[43]. Compound **6c**, at

the dose tested, was neither able to decrease the focal susceptibility to generate seizures, nor to block the secondary generalization. In fully kindled rats, 2 h following administration of compound **6c**, the afterdischarge threshold, defined as the lowest current intensity inducing an electrographic response ≥ 3 sec, was not changed compared to vehicle treated animals (Wilcoxon test, p = 0.125, Fig. 4A). The duration of the afterdischarge on EEG at the threshold intensity and the behavioral seizure response (on the Racine's scale: stage 0: arrest, normal behavior; stage 1: facial twitches; stage 2: chewing, head nodding; stage 3: forelimb clonus; stage 4: rearing, falling on forelimbs; stage 5: rearing, falling on side or back, rolling) were also unchanged compared to vehicle treated rats (p = 0.3125 and p = 0.75, Figs. 4B and C respectively). Similar results were recently published with compound **2**[44], in line with what we observed with compound **6c**.

The cardiovascular safety of compound **6c** was evaluated in freely moving, conscious male spontaneously hypertensive rats (SHRs) equipped with a telemetry system allowing noninvasive monitoring of mean arterial pressure (MAP), heart rate (HR) and electrocardiogram. The compound was administered as a single oral dose of 100 mg/kg in the morning at the end of the wake phase of the animals. MAP was decreased ~12 mmHg by Compound **6c** and it returned to baseline values within 18 hours (Fig. 5A). A slight decrease in HR was observed which returned to baseline values within 6 hours (data not shown). On the electrocardiogram, compound **6c** increased PR-intervals (indicative of AV-block type I, Fig. 5B) and induced AV-blocks type II (Wenckebach and Mobitz II). In spite of the low IC_{50}-value of compound **6c** on the hERG channel, no QT-prolongation was observed. If we assume that exposure in these animals should be similar to what we observed in the blood-brain pharmacokinetic experiments we run in Wistar rats (Table 9), free concentration at 1h (C_u = 37 nM) corresponds to IC_{50}-values on $Ca_v3.1$ and $Ca_v3.2$, both present in the heart, and remain much below the IC_{50}-value on the hERG channel.

CONCLUSIONS

In conclusion, we have developed a series of dihydropyrazole compounds as potent, selective and brain penetrant TTCC blockers. The lead compound of this series, dihydropyrazole **6c**, was used as a tool compound to evaluate potential efficacy for epilepsy indications and cardiovascular safety; it showed good efficacy and minimal safety issues. Issues related to solubility and intellectual property led us to stop the development of this class of compounds.

EXPERIMENTAL SECTION

Chemistry. All final compounds were analyzed by 1H-NMR and LC-MS, and were found to be > 95% pure by these analytical methods. Description of general methods, especially of gradients used in LC-MS, can be found in the supporting information.

(*E*)-1-(4-Bromophenyl)-3-(4-fluorophenyl)prop-2-en-1-one (3a). To a solution of 4-fluorobenzaldehyde (3.00 g, 24.2 mmol) in ethanol (50 ml) was added aqueous 30% KOH (10 ml) during 2 minutes, and the mixture was stirred for 5 minutes at 23 °C. A solution of 1-(4-bromophenyl)ethan-1-one (4.80 g; 24.2mmol) in diethyl ether (20 ml) was added during 5 minutes at rt and the mixture was stirred for 50 minutes. The suspension was poured into ice - water and aqueous 1N HCl (150 ml) was added to maintain the pH = 1. The precipitate was filtered off, washed with cold water (100 ml) and stirred in ethanol (75 ml) for 1 h. The crude product was filtered off and dried to afford 5.6 g (76%) of a yellowish solid. ^{1}H NMR (400 MHz, CDCl3) δ 7.90 (d, J = 8.5 Hz, 2H), 7.80 (d, J =15.7 Hz, 1H), 7.63-7.70 (m, 4H), 7.43 (d, J = 15.7 Hz, 1H), 7.14 (t, J = 8.6 Hz, 2H). LC-MS (method A): t_r = 1.13 min; [M+H]+: not visible.

3-(4-Bromophenyl)-5-(4-fluorophenyl)-4,5-dihydro-1H-pyrazole (4a). To a solution of **3a** (1.43 g, 4.70 mmol) in toluene (60 ml) was added hydrazine hydrate (0.75 ml, 15.5 ml) and the mixture was stirred at rt for 21 h. The solvent was evaporated *in vacuo* and crude product (1.52 g of brown oil) was used in the next step without purification. LC-MS (method A): t_r = 1.05 min; $[M+H]^+$: not visible.

3-(4-Bromophenyl)-5-(4-fluorophenyl)-*N*-phenyl-4,5-dihydro-1H-pyrazole-1-carboxamide (5a). To a solution of **4a** (1.52 g, 4.76 mmol) in toluene (120 ml) was added phenylisocyanate (568 mg; 4.77 mmol) and Et_3N (3 drops) and the mixture was stirred at 90 °C for 40 minutes. The solvent was evaporated *in vacuo* and crude was purified by automated flash chromatography (Büchi Sepacore, 50 g cartridge, solvent A: heptane, solvent B: ethyl acetate, gradient in % B: 2 to 10, flow rate: 30ml/min) to afford 0.9 g of a yellowish foam. ^{1}H NMR (400 MHz, CDCl3) δ 8.08 (s, 1H), 7.59-7.46 (m, 4H), 7.52 (d, J = 8.0 Hz, 2H), 7.28-7.33 (m, 4H), 7.02-7.08 (m, 3H), 5.60 (dd, J_1 = 12.2 Hz, J_2 = 5.5 Hz, 1H), 3.83 (dd, J_1 = 17.7 Hz, J_2 = 12.2 Hz, 1H), 3.19 (dd, J_1 = 17.8 Hz, J_2 = 5.5 Hz, 1H). ^{13}C NMR (100 MHz, $CDCl_3$) δ 163.5, 161.0, 151.4, 150.7, 138.3, 138.0, 132.0, 130.0, 128.9, 127.9, 127.4, 124.7, 123.1, 119.0, 115.8. LC-MS (method A): t_r = 1.16 min; $[M+H]^+$: 437.67.

Following compounds have been synthesized from appropriate starting materials according to the procedures described for compound **5a**:

3-(4-Bromophenyl)-*N*,5-bis(4-fluorophenyl)-4,5-dihydro-1H-pyrazole-1-carboxamide (5b). ^{1}H NMR (400 MHz, $CDCl_3$) δ 8.02 (s, 1H), 7.59-7.64 (m, 4H), 7.47 (dd, J_1 = 9.0 Hz, J_2 = 4.8 Hz, 2H), 7.28-7.31 (m, 2H), 7.05 (t, J = 8.6 Hz, 2H), 7.02 (t, J = 8.6 Hz, 2H), 5.59 (dd, J_1 = 12.2 Hz, J_2 = 5.9 Hz, 1H), 3.85 (dd J_1 = 17.7 Hz, J_2= 12.1 Hz, 1H), 3.20 (dd, J_1 = 17.8 Hz, J_2 = 5.9 Hz, 1H). LC-MS (method A): t_r = 1.16 min; $[M+H]^+$: 455.82.

3-(4-Bromophenyl)-*N*-(3-fluorophenyl)-5-(4-fluorophenyl)-4,5-dihydro-1H-pyrazole-1-carboxamide (5c). ^{1}H NMR (400 MHz, $CDCl_3$) δ 8.14 (s, 1H), 7.49-7.55 (m, 4H), 7.46 (dt, J_1 = 11.2 Hz, J_2 = 2.1 Hz, 1H), 7.27-7.31 (m, 2H), 7.23 (t, J = 6.6 Hz, 1H), 7.16 (d, J = 8.5 Hz, 1H), 7.05 (t, J = 8.6 Hz, 1H), 6.75 (td, J_1 = 8.3 Hz, J_2 = 2.3 Hz, H), 5.59 (dd, J_1 = 12.1 Hz, J_2 = 5.8 Hz, 1H), 3.85 (dd, J_1 = 17.8 Hz, J_2 = 12.2 Hz, 1H), 3.20 (dd, J_1 = 17.8 Hz, J_2 = 5.8 Hz, 1H). LC-MS (method A): t_r = 1.16 min; $[M+H]^+$: 455.70.

3-(4-Bromophenyl)-*N*-(2-fluorophenyl)-5-(4-fluorophenyl)-4,5-dihydro-1H-pyrazole-1-carboxamide (5d). ^{1}H NMR (400 MHz, $CDCl_3$) δ 8.38 (d, J = 2.6 Hz, 1H), 8.22 (t, J = 8.1 Hz, 1H), 7.59-7.64 (m, 4H), 7.29-7.32 (m, 2H), 6.95-7.17 (m, H), 5.60 (dd, J_1 = 12.1 Hz, J_2 = 5.8 Hz, 1H), 3.85 (dd, J_1 = 17.7 Hz, J_2 = 12.1 Hz, 1H), 3.21 (dd, J_1 = 17.7 Hz, J_2 = 5.8 Hz, 1H). LC-MS (method A): t_r = 1.18 min; $[M+H]^+$: 455.91.

3-(4-Bromophenyl)-5-(4-fluorophenyl)-*N*-(4-methoxyphenyl)-4,5-dihydro-1H-pyrazole-1-carboxamide (5e). ^{1}H NMR (300 MHz, $CDCl_3$) δ 7.91 (s, 1H), 7.53-7.64 (m, 4H), 7.39 (d, J = 9.0 Hz, 2H), 7.23-7.29 (m, 2H), 7.02 (t, J = 8.7 Hz, 2H), 6.83 (d, J = 9.3 Hz, 2H), 5.56 (dd, J_1 = 12.0 Hz, J_2 = 5.90 Hz, 1H), 3.80 (dd, J_1 = 17.9 Hz, J_2 = 12.3 Hz, 1H), 3.77 (s, 3H), 3.16 (dd, J_1 = 17.6 Hz, J_2 = 5.9 Hz, 1H). LC-MS (method A): t_r = 1.15 min; $[M+H]^+$: 467.79.

3-(4-Bromophenyl)-*N*-(4-ethylphenyl)-5-(4-fluorophenyl)-4,5-dihydro-1H-pyrazole-1-carboxamide (5f) . ^{1}H NMR (400 MHz, $CDCl_3$) δ 8.02 (s, 1H), 7.58-7.64 (m, 4H), 7.42 (d, J = 8.4 Hz, 2H), 7.27-7.31 (m, 2H), 7.14 (d, J = 8.3 Hz, 2H), 7.04 (t, J = 8.6 Hz, 2H), 5.60 (dd, J_1 = 12.1 Hz J_2 = 5.8 Hz, 1H), 3.83 (dd, J_1 = 17.7 Hz, J_2 = 12.2 Hz, 1H), 3.18 (dd, J_1 = 17.7 Hz, J_2 = 5.8 Hz, 1H), 2.62 (q J = 7.8 Hz, 2H), 1.23 (t, J = 7.6 Hz, 3H). LC-MS (method A): t_r = 1.20 min; $[M+H]^+$: 466.23.

3-(4-Bromophenyl)-*N*-cyclohexyl-5-(4-fluorophenyl)-4,5-dihydro-1H-pyrazole-1-carboxamide (5g). ^{1}H NMR (400 MHz, $CDCl_3$) δ 7.54-7.59 (m, 4H), 7.28 (s, 1H), 7.24 (dd, J_1 = 8.6 Hz, J_2 = 5.3 Hz, 2H), 7.02 (t, J = 8.6 Hz, 2H), 5.89-5.93 (m, 1H), 5.50 (dd, J_1 = 12.2 Hz, J_2 = 6.0 Hz, 1H), 3.75 (dd, J_1 = 17.6 Hz, J_2 = 12.2 Hz, 1H), 3.59-3.69 (m, 1H), 3.11 (dd, J_1 = 17.6 Hz, J_2 = 6.0 Hz, 1H), 1.88-2.03 (m, 2H), 1.70-1.77 (m, 2H), 1.28-1.40 (m, 4H). LC-MS (method A): t_r = 1.16 min; $[M+H]^+$: 444.09.

3-(4-Bromophenyl)-5-(4-fluorophenyl)-*N*-isopropyl-4,5-dihydro-1H-pyrazole-1-carboxamide (5h). ^{1}H NMR (400 MHz, $CDCl_3$) δ 7.53-7.59 (m, 4H), 7.28 (s, 1H), 7.24 (dd, J_1 = 7.6 Hz, J_2 = 5.6 Hz, 2H), 7.02 (t, J = 8.4 Hz, 2H), 5.86 (d, J = 7.9 Hz, 1H), 5.50 (dd, J_1 = 12.3 Hz, J_2 = 6.0 Hz, 1H), 4.15 (q, J = 7.1 Hz, 1H), 3.95-4.00 (m, 1H), 3.75 (dd, J_1= 17.8 Hz, J_2 = 12.2 Hz, 1H), 3.10 (dd, J_1 = 17.7 Hz, $J2$ = 5.9 Hz, 1H), 1.23 (dd, J_1 = 6.1 Hz, J_2 = 3.6 Hz, 6H). LC-MS (method A): t_r = 1.10 min; $[M+H]^+$: 403.99.

(3-(4-Bromophenyl)-5-(4-fluorophenyl)-4,5-dihydro-1H-pyrazol-1-yl)(phenyl)methanone (5i). ^{1}H NMR (400 MHz, $CDCl_3$) δ 8.01 (d, J = 7.4 Hz, 2H), 7.45-7.60 (m, 7H), 7.33 (dd, J_1 = 8.5 Hz, J_2 = 5.3 Hz, 2H), 7.06 (t, J = 8.6 Hz, 2H), 5.84 (dd, J_1 = 11.8 Hz, J_2 = 5.2 Hz, 1H), 3.80 (dd, J_1 = 17.7 Hz, J_2 = 11.9 Hz, 1H), 3.18 (dd, J_1 = 17.7 Hz, J_2 = 5.2 Hz, 1H). LC-MS (method A): t_r = 1.14 min; $[M+H]^+$: 422.89.

3-(4-Bromophenyl)-5-(4-fluorophenyl)-*N*-phenethyl-4,5-dihydro-1H-pyrazole-1-carboxamide (5j). ^{1}H NMR (400 MHz, $CDCl_3$) δ 7.56 (d, J = 8.3 Hz, 2H), 7.52 (d, J = 8.3 Hz, 2H), 7.23-7.36 (m, 7H), 7.04 (t, J = 8.3 Hz, 2H), 6.14 (t, J = 5.6 Hz, 1H), 5.51 (dd, J_1 = 12.1 Hz, J_2 = 6.0 Hz, 1H), 3.75 (dd, J_1 = 17.6 Hz, J_2 = 12.2 Hz, 1H), 3.56 (m, 2H), 3.11 (dd, J_1 = 17.6 Hz, J_2 = 5.9 Hz, 1H), 2.81-2.95 (m, 2H). LC-MS (method A): t_r = 1.15 min; $[M+H]^+$: 468.66.

3-(4-Bromophenyl)-5-(4-fluorophenyl)-*N*-(pyridin-4-yl)-4,5-dihydro-1H-pyrazole-1-carboxamide (5k). ^{1}H NMR (400 MHz, $CDCl_3$) δ 8.45 (d, J = 5.4 Hz, 2H), 8.33 (s, 1H), 7.75-7.80 (m, 2H), 7.47-7.54 (m, 5H), 7.30-7.32 (m, 2H), 7.07 (t, J = 8.6 Hz, 2H), 5.59 (dd, J_1 = 12.0 Hz, J_2 = 5.7 Hz, 1H), 3.91 (dd, J_1 = 17.9 Hz, J_2 = 12.0 Hz, 1H), 3.28 (dd, J_1 = 17.8 Hz, J_2 = 5.6 Hz, 1H). LC-MS (method A): t_r = 0.87 min; $[M+H]^+$: 361.26.

3-(4-Bromophenyl)-5-(4-fluorophenyl)-*N*-(pyridin-2-yl)-4,5-dihydro-1H-pyrazole-1-carboxamide (5l). ^{1}H NMR (400 MHz, $CDCl_3$) δ 8.93-9.06 (m, 1H), 8.28 (d, J = 4.5 Hz, 1H), 8.14 (d, J = 8.5 Hz, 1H), 7.75-7.83 (m, 2H), 7.67 (t, J = 7.6 Hz, 1H), 7.44-7.50 (m, 3H), 7.31 (dd, J_1 = 8.6 Hz, J_2 = 5.3 Hz, 2H), 7.06 (t, J = 8.6 Hz, 2H), 7.00 (t, J = 6.1 Hz, 1H), (m, 1H), 6.83 (s), 5.60 (dd, J_1 = 12.0 Hz, J_2 = 5.5 Hz, 1H), 3.88 (dd, J_1 = 17.7 Hz, J_2 = 12.0 Hz, 1H), 3.25 (dd, J_1 = 17.7 Hz, J_2 = 5.5 Hz, 1H). LC-MS (method A): t_r = 0.92 min; $[M+H]^+$: 361.32.

3-(4-Bromophenyl)-N,5-bis(4-fluorophenyl)-4,5-dihydro-1H-pyrazole-1-carbothioamide (5m). ^{1}H NMR (400 MHz, $CDCl_3$) δ 9.12 (s, 1H), 7.66 (d, J = 8.3 Hz, 2H), 7.61 (d, J = 8.0 Hz, 2H), 7.56 (dd, J_1 = 7.7 Hz, J_2 = 5.0 Hz, 2H), 7.26 (dd, J_1 = 12.7 Hz, J_2 = 5.9 Hz, 2H), 7.02-7.08 (m, 4H), 6.16 (dd, J_1 = 3.4 Hz, J_2 = 11.6 Hz, 1H), 3.87 (dd, J_1 = 17.8 Hz, J_2 = 11.7 Hz, 1H), 3.20 (dd, J_1 = 17.8 Hz, J_2 = 3.5 Hz, 1H). LC-MS (method A): t_r = 1.18 min; $[M+H]^+$: 471.92.

***N*,5-Bis(4-fluorophenyl)-3-phenyl-4,5-dihydro-1H-pyrazole-1-carboxamide (6a).** ^{1}H NMR (400 MHz, $CDCl_3$) δ 8.08 (s, 1H), 7.75-7.80 (m, 2H), 7.46-7.52 (m, 5H), 7.27-7.33 (m, 2H), 7.05 (t, J = 8.6 Hz, 2H), 7.00 (t, J = 8.6 Hz, 2H), 5.59 (dd, J_1 = 12.1 Hz, $J2$ = 5.8 Hz, 1H), 3.88 (dd, $J1$ = 17.7 Hz, $J2$ = 12.1 Hz, 1H), 3.24 (dd, $J1$ = 17.7 Hz, J_2 = 5.7 Hz, 1H). LC-MS (method B): t_r = 1.00 min; $[M+H]^+$: 378.12.

***N*,5-Bis(4-fluorophenyl)-3-methyl-4,5-dihydro-1H-pyrazole-1-carboxamide (6b).** ^{1}H NMR (400 MHz, $CDCl_3$) δ 7.91 (s, 1H), 7.42-7.45 (m, 2H), 7.24 (dd, J_1 = 8.6 Hz, J_2 = 5.3 Hz, 2H),

7.04 (t, J = 8.6 Hz, 2H), 6.97 (t, J = 8.6 Hz, 2H), 5.40 (dd, J_1 = 11.9 Hz, J_2 = 5.9 Hz, 1H), 3.29-3.68 (m, 1H), 2.77 (dd, J_1 = 18.2 Hz, J_2 = 5.9 Hz, 1H), 2.11 (s, 3H). LC-MS (method A): t_r = 1.03 min; $[M+H]^+$: 316.42.

***N*,5-Bis(4-fluorophenyl)-3-(pyridin-4-yl)-4,5-dihydro-1H-pyrazole-1-carboxamide (6c).** ^{1}H NMR (400 MHz, CDCl3) δ: 8.74 (dd, J1 = 6.1 Hz, J2 = 1.6 Hz, 2H), 8.03 (s, 1H), 7.60 (dd, J1 = 6.1 Hz, J2 = 1.6 Hz, 2H), 7.46 (dd, J_1 = 9.3 Hz, J_2 = 4.8 Hz, 2H), 7.27-7.30 (m, 2H), 7.05 (t, J = 8.5 Hz, 2H), 7.00 (t, J = 8.5 Hz, 2H), 5.61 (dd, J_1 = 12.6 Hz, J_2 = 6.4 Hz, 1H), 3.85 (dd, J_1 = 18.2 Hz, J_2 = 13.1 Hz, 1H), 3.21 (dd, J_1 = 18.4 Hz, J_2 = 6.4 Hz, 1H). ^{13}C NMR (100 MHz, $CDCl_3$) δ 163.3, 161.3, 159.9, 157.9, 151.2, 150.4, 149.5, 138.2, 137.7, 134.0, 127.4, 127.3, 121.0, 120.9, 120.2, 116.3, 116.1, 115.9, 115.6, 60.3, 42.2. LC-MS (method A): t_r = 0.87 min; $[M+H]^+$: 379.43.

***(R)*-*N*,5-Bis(4-fluorophenyl)-3-(pyridin-4-yl)-4,5-dihydro-1H-pyrazole-1-carboxamide ((*R*)-6c) and *(S)*-*N*,5-Bis(4-fluorophenyl)-3-(pyridin-4-yl)-4,5-dihydro-1H-pyrazole-1-carboxamide ((*S*)-6c).** Compound **6c** was separated by HPLC using a chiral stationary phase (Diacel ChiralPak IB 5 μm column, 30 x 250 mm, EtOH / heptane 4:6 with 0.05% Et_2NH, 34 ml/min, 15 min). Compound **(*R*)-6c** eluted at 11.8 min, compound **(*S*)-6c** at 8.68 min. ^{1}H-NMR and LC-MS spectra for each compound was identical to **6c**. Enantiomeric purity > 95% by analytical HPLC (Diacel ChiralPak IB 5 μm column, 4.6 x 250 mm, EtOH / heptane 4:6 with 0.05% Et_2NH, 0.8 ml/min, 15 min). $[\alpha]_D$ (c = 1, $CHCl_3$): +81.2 ° for **(*R*)-6c**, and -85.8 ° for **(*S*)-6c**. Absolute configuration determined by analogy to compounds **(*R*)-11h** and **(*S*)-11h**.

4-(5-(4-Fluorophenyl)-1-((4-fluorophenyl)carbamoyl)-4,5-dihydro-1H-pyrazol-3-yl)pyridine 1-oxide (6d). A solution of *N*,5-bis(4-fluorophenyl)-3-(pyridin-4-yl)-4,5-dihydro-1H-pyrazole-1-carboxamide (100 mg, 0.26 mmol) and MCPBA (68 mg, 0.40 mmol) in CH_2Cl_2

(6 ml) was stirred at rt for 3 h. The mixture was diluted with aqueous 1N NaOH and ethyl acetate. The layers were separated, the aqueous phase was washed with CH_2Cl_2 and the combined organic layers were dried over $MgSO_4$, filtrated off and evaporated *in vacuo*. The crude was purified by automated flash chromatography (Büchi Sepacore, 5 g cartridge, solvent A: CH_2Cl_2, solvent B: 7M NH_3 in MeOH, gradient in %B: 0 to 2, flow rate: 12.5 ml/min) to afford 92 mg (89%) of an yellowish foam. ^{1}H NMR (400 MHz, $CDCl_3$) δ 8.27 (d, J = 7.2 Hz, 2H), 7.96 (s, 1H), 7.62 (d, J = 7.2 Hz, 2H), 7.45 (dd, J_1 = 9.0 Hz, J_2 = 4.5 Hz, 2H), 7.28-7.45 (m, 2H), 7.06 (t, J = 8.6 Hz, 2H), 7.01 (t, J = 8.7 Hz, 2H), 5.64 (dd, J_1 = 12.3 Hz, J_2 = 6.0 Hz, 1H), 5.32 (s, 1 H), 3.82 (dd, J_1 = 17.7 Hz, J_2 = 12.3 Hz, 1H), 3.18 (m, 1H). LC-MS (method A): t_r = 1.02 min; $[M+H]^+$: 395.59.

***N*-(4-Fluorophenyl)-5-methyl-3-phenyl-4,5-dihydro-1H-pyrazole-1-carboxamide (6e).** ^{1}H NMR (400 MHz, $CDCl_3$) δ 8.00 (s, 1H), 7.73-7.76 (m, 2H), 7.44-7.54 (m, 4H), 7.28 (s, 1H), 7.04 (t, J = 8.6 Hz, 2H), 4.71 (m, 1H), 3.54 (dd, J_1 = 17.3 Hz, J_2 = 11.1 Hz, 1H), 2.91 (m, 1H), 1.50 (d, J = 6.3 Hz, 3H). LC-MS (method A): t_r = 1.03 min; $[M+H]^+$: 298.00.

***N*-(4-Fluorophenyl)-5-(4-(methylsulfonyl)phenyl)-3-phenyl-4,5-dihydro-1H-pyrazole-1-carboxamide (6f).** ^{1}H NMR (400 MHz, $CDCl_3$) δ 8.08 (s, 1H), 7.94 (d, J = 8.3 Hz, 2H), 7.76 (dd, J_1 = 8.0 Hz, J_2 = 4.0 Hz, 2H), 7.53 (d, J = 8.0 Hz, 2H), 7.41-7.53 (m, 5H), 7.00 (t, J = 8.0 Hz, 2H), 5.65 (dd, J_1 = 12.2 Hz, J_2 = 6.0 Hz, 1H), 3.93 (dd, J_1 = 17.8 Hz, J_2 = 12.2 Hz, 1H), 3.22 (dd, J_1 = 17.8 Hz, J_2 = 6.2 Hz, 1H), 3.04 (s, 3H). LC-MS (method C): t_r = 4.42 min; $[M+H]^+$: 438.30.

***N*-(4-Fluorophenyl)-5-(4-(methylsulfonyl)phenyl)-3-(pyridin-4-yl)-4,5-dihydro-1H-pyrazole-1-carboxamide (6g).** ^{1}H NMR (400 MHz, $CDCl_3$) δ 9.34 (s, 1H), 8.70 (d, J = 5.8 Hz, 2H), 7.92 (d, J = 8.3 Hz, 2H), 7.86 (d, J = 5.8 Hz, 2H), 7.56-7.65 (m, 2H), 7.54 (d, J = 8.3 Hz,

2H), 7.12 (t, J = 8.0 Hz, 2H), 5.70 (dd, J_1 = 12.4 Hz, J_2 = 6.2 Hz, 1H), 3.94 (dd, J_1 = 18.1 Hz, J_2 = 12.3 Hz, 1H), 3.11-3.29 (m, 4H). LC-MS (method C): t_r = 2.87 min; $[M+H]^+$: 439.40.

1-Phenyl-4-((tetrahydro-2H-pyran-2-yl)oxy)but-2-yn-1-one (7a). To a solution of 2-(prop-2-yn-1-yloxy)tetrahydro-2H-pyran (2.23 g, 15.9 mmol) in THF (40 ml) was added at -78°C n-BuLi (1.6 M in THF, 9.95 ml, 15.9 mmol) and the mixture was stirred at this temperature for 1 h. A solution of *N*-methoxy-*N*-methylbenzamide (2.5 g, 15.2 mmol) in THF (10 ml) was added and the mixture was stirred at rt for 1 h. The mixture was diluted with saturated aqueous NH_4Cl and ethyl acetate. The layers were separated, the aqueous phase was washed with ethyl acetate, and the combined organic layers were dried over $MgSO_4$, filtrated off and evaporated *in vacuo*. The crude was purified by automated flash chromatography (Büchi Sepacore, 70 g cartridge, solvent A: heptane, solvent B: ethyl acetate, gradient in %B: 1 to 3, flow rate: 50 ml/min) to afford 3.0 g (77%) of an yellowish oil. ^{1}H NMR (400 MHz, $CDCl_3$) δ 8.17 (d, J = 7.5 Hz, 2H), 7.64 (t, J = 7.1 Hz, 1H), 7.52 (t, J = 7.8 Hz, 2H), 4.92 (t, J = 3.3 Hz, 1H), 4.57 (s, 2H), 3.85-3.95 (m, 1H), 3.56-3.64 (m, 1H), 1.51-1.95 (m, 6H). LC-MS (A): t_r = 1.04 min; $[M+H]^+$: 245.38.

(*E/Z*)-3-(4-Fluorophenyl)-1-phenyl-4-((tetrahydro-2H-pyran-2-yl)oxy)but-2-en-1-one (8a). To a solution of $CuBr{\cdot}Me_2S$ (1.03 g, 4.9 mmol) in THF (15 ml) was added at -78 °C (4-fluorophenyl)magnesium bromide (1 M in THF, 9.8 ml, 9.8 mmol), and the mixture was stirred at this temperature for 1.5 h. The solution of **7a** (1 g, 4.1 mmol) was added in THF (5 ml) and the reaction was stirred at -78 °C for 3 h. The mixture was diluted at 0 °C with saturated aqueous NH_4Cl and ethyl acetate. The layers were separated, the aqueous phase was washed with ethyl acetate, and the combined organic layers were dried over $MgSO_4$, filtrated off and evaporated *in vacuo*. The crude was purified by automated flash chromatography (Büchi Sepacore, 20 g cartridge, solvent A: heptane, solvent B: ethyl acetate, gradient in %B: 1 to 5, flow rate: 35

ml/min) to afford 182 mg (13%) of an yellowish oil. LC-MS (method A): t_r =1.10 min; $[M+H]^+$: 341.32.

5-(4-Fluorophenyl)-3-phenyl-5-(((tetrahydro-2H-pyran-2-yl)oxy)methyl)-4,5-dihydro-1H-pyrazole (9a). A solution of **8a** (177 mg, 0.52 mmol) and hydrazine monohydrate (53 mg, 1.04 mmol) in EtOH (3 ml) was stirred in microwave at 150°C for 1h. The solvent was evaporated *in vacuo* and crude product (184 mg of yellowish oil) was used in the next step without purification. LC-MS (method A): t_r = 1.08 min; $[M+H]^+$: 355.43.

***N*,5-Bis(4-fluorophenyl)-3-phenyl-5-(((tetrahydro-2H-pyran-2-yl)oxy)methyl)-4,5-dihydro-1H-pyrazole-1-carboxamide (10a).** A solution of **9a** (184 mg, 0.52 mmol), 1-fluoro-4-isocyanatobenzene (71 mg, 0.52 mmol) and Et_3N (10 mg, 0.1 mmol) in toluene (5 ml) was stirred at 90 °C overnight. Additional 1-fluoro-4-isocyanatobenzene was added (28 mg, 0.20 mmol) and the reaction was stirred for 2 h. The mixture was diluted at rt with ethyl acetate, and aqueous HCl (1 M). The layers were separated, the organic phase was washed with saturated aqueous $NaHCO_3$. The layers were separated and the org. layer was dried over $MgSO_4$, filtrated off and evaporated *in vacuo*. The crude was purified by automated flash chromatography (Büchi Sepacore, 5 g cartridge, solvent A: heptane, solvent B: ethyl acetate, gradient in %B: 1 to 4, flow rate: 15 ml/min) to afford 106 mg (41%) of an yellowish resin. LC-MS (method A): t_r = 1.17 min; $[M+H]^+$: not visible.

***N*,5-Bis(4-fluorophenyl)-5-(hydroxymethyl)-3-phenyl-4,5-dihydro-1H-pyrazole-1-carboxamide (11a).** A solution of **10a** (100 mg, 0.2 mmol) and PTSA (2.9 mg, 0.01 mmol) in Et_2O (1 ml) was stirred at 0 °C for 1.5 h. The mixture was diluted at rt with ethyl acetate, and saturated aqueous $NaHCO_3$. The layers were separated, the org. phase was washed with saturated aqueous NaCl. The layers were separated and the organic layer was dried over $MgSO_4$, filtrated

off and evaporated *in vacuo*. The crude was purified by flash chromatography (Büchi Sepacore, 2 g cartridge, solvent A: heptane, solvent B: ethyl acetate, gradient in %B: 2, flow rate: 15 ml/min) to afford 40 mg (48%) of an colorless foam. ^{1}H NMR (400 MHz, $CDCl_3$) δ 8.31 (s, 1H), 7.68-7.75 (m, 2H), 7.43-7.53 (m, 5H), 7.32 (dd, J_1 = 8.9 Hz, J_2 = 5.1 Hz, 2H), 7.08 (t, J = 8.6 Hz, 2H), 7.04 (t, J = 8.7 Hz, 2H), 4.89-5.26 (m, 1H), 4.50 (d, J = 12.3 Hz, 1H), 4.24 (d, J = 12.3 Hz, 1H), 3.50 (d, J = 18.2 Hz, 1H), 3.38 (d, J = 17.8 Hz, 1H). LC-MS (method A): t_r = 1.09 min; $[M+H]^+$: 407.98.

Following compounds have been synthesized from appropriate starting materials according to the procedures described for compound **11a**:

***N*-(4-Fluorophenyl)-5-(2-hydroxyethyl)-3,5-diphenyl-4,5-dihydro-1H-pyrazole-1-carboxamide (11b).** ^{1}H NMR (500 MHz, $CDCl_3$) δ 8.30 (s, 1H), 7.70-7.74 (m, 2H), 7.48 (dd, J_1 = 9.1 Hz, J_2 = 4.8 Hz, 2H), 7.43-7.47 (m, 3H), 7.35-7.40 (m, 4H), 7.26-7.30 (m, 1H), 7.00 (t, J = 8.5 Hz, 2H), 3.87-3.99 (m, 2H), 3.80 (d, J = 21.1 Hz, 1H), 3.48 (d, J = 17.8 Hz, 1H), 3.13 (dt, J_1 = 14.2 Hz, J_2 = 5.9 Hz, 1H), 2.60-2.67 (m, 1H). LC-MS (method B): t_r = 0.93 min; $[M+H]^+$: 404.17.

N-(4-Fluorophenyl)-5-(2-hydroxyethyl)-5-(4-(2-methoxyethoxy)phenyl)-3-phenyl-4,5-dihydro-1H-pyrazole-1-carboxamide (11c). ^{1}H NMR (400 MHz, $CDCl_3$) δ 8.28 (s, 1H), 7.23 (dd, J_1 = 5.2 Hz, J_2 = 2.8 Hz, 2H), 7.43-7.50 (m, 5H), 7.25-7.31 (m, 2H), 7.00 (t, J = 8.4 Hz, 2H), 6.92 (t, J = 9.2 Hz, 2H), 4.11 (t, J = 2.2 Hz, 2H), 3.83-3.96 (m, 3H), 3.74 (t, J = 4.8 Hz, 2H), 3.45 (s, 3H), 3.44 (d, J = 18.0 Hz, 1H), 3.05-3.12 (m, 1H), 2.56-2.63 (m, 1H). LC-MS (method C): t_r = 4.61 min; $[M+H]^+$: 478.33.

5-(4-(2-(Dimethylamino)ethoxy)phenyl)-*N*-(4-fluorophenyl)-5-(2-hydroxyethyl)-3-phenyl-4,5-dihydro-1H-pyrazole-1-carboxamide (11d). ^{1}H NMR (400 MHz, $CDCl_3$) δ 8.28 (s, 1H),

7.22 (dd, J_1 = 6.0 Hz, J_2 = 2.4 Hz, 2H), 7.42-7.50 (m, 5H), 7.25-7.32 (m, 2H), 7.00 (t, J = 8.8 Hz, 2H), 6.90 (t, J = 8.8 Hz, 2H), 4.07 (t, J = 5.2 Hz, 2H), 3.83-3.97 (m, 3H), 3.44 (d, J = 18.0 Hz, 1H), 3.05-3.12 (m, 1H), 2.76 (t, J = 5.2 Hz, 2H), 2.56-2.63 (m, 1H), 2.36 (s, 6H). LC-MS (method C): t_r = 3.59 min; $[M+H]^+$: 491.49.

***N*-(4-Fluorophenyl)-5-(2-hydroxyethyl)-3-(pyridin-4-yl)-5-(p-tolyl)-4,5-dihydro-1H-pyrazole-1-carboxamide (11e).** ^{1}H NMR (400 MHz, $CDCl_3$) δ 8.69 (d, J = 4.6 Hz, 2H), 8.22 (s, 1H), 7.53 (d, J = 6.0 Hz, 2H), 7.42-7.50 (m, 2H), 7.12-7.27 (m, 4H), 6.99 (t, J = 8.4 Hz, 2H), 3.79-4.03 (m, 2H), 3.91 (d, J = 17.6 Hz, 1H), 3.39 (d, J = 18.0 Hz, 1H), 3.03-3.15 (m 1H), 2.56-2.67 (m, 1H), 2.32 (s, 3H). LC-MS (method C): t_r = 3.22 min; $[M+H]^+$: 419.39.

(*R*)-*N*-(4-Chlorophenyl)-5-(2-hydroxyethyl)-5-(4-methoxyphenyl)-3-(pyridin-3-yl)-4,5-dihydro-1H-pyrazole-1-carboxamide (11f). ^{1}H NMR (400 MHz, $CDCl_3$) δ 8.93 (s, 1H), 8.66 (broad d, J = 4.7 Hz, 1H), 8.30 (s, 1H), 8.03 (broad d, J = 8.0 Hz, 1H), 7.47 (d, J = 8.5 Hz, 2H), 7.39 (dd, J_1 = 7.9 Hz, J_2 = 5.0 Hz, 1H), 7.27 (m, 4H), 6.90 (d, J = 8.6 Hz, 2H), 3.93(d, J = 17.5 Hz, 1H), 3.82-3.97 (m, 2H), 3.80 (s, 3H), 3.43 (d, J = 17.9 Hz, 1H), 3.08 (dt, J_1 = 16.0 Hz, J_2 = 6.4 Hz, 1H), 2.58-2.67 (m, 1H), 1.95 (broad s, 1H). LC-MS (method B): t_r = 0.79 min; $[M+H]^+$: 451.11.

***N*-(4-Fluorophenyl)-5-(2-hydroxyethyl)-5-(4-(methylsulfonyl)phenyl)-3-phenyl-4,5-dihydro-1H-pyrazole-1-carboxamide (11g)**. ^{1}H NMR (400 MHz, $CDCl_3$) δ 8.28 (s, 1H), 7.95 (d, J = 8.4 Hz, 2H), 7.69-7.74 (m, 2H), 7.59 (d, J = 8.4 Hz, 2H), 7.42-7.50 (m, 5H), 7.02 (t, J = 8.4 Hz, 2H), 4.0 (d, J = 17.6 Hz, 1H), 3.86-4.02 (m, 2H), 3.39 (d, J = 18 Hz, 1H), 3.03-3.15 (m 1H), 3.06 (s, 3H), 2.56-2.67 (m, 1H). LC-MS (method C): t_r = 4.13 min; $[M+H]^+$: 482.19.

***N*-(4-Bromophenyl)-5-(2-hydroxyethyl)-5-(4-methoxyphenyl)-3-(pyridin-3-yl)-4,5-dihydro-1H-pyrazole-1-carboxamide (11h).** ^{1}H NMR (400 MHz, $CDCl_3$) δ 8.92 (d, J = 1.8 Hz, 1H),

8.65 (dd, J_1 = 4.8 Hz, J_2 = 1.5 Hz, 1H), 8.29 (s, 1H), 8.02 (dt, J_1 = 8.0 Hz, J_2 = 1.8 Hz, 1H), 7.35-7.46 (m, 5H), 7.28 (d, J = 9.0 Hz, 2H), 6.90 (d, J = 8.9 Hz, 2H), 3.95(d, J = 18.2 Hz 1H), 3.81-3.96 (m, 2H), 3.80 (s, 3H), 3.43 (d, J = 17.9 Hz, 1H), 3.08 (dt, J_1 = 14.3 Hz, J_2 = 5.7 Hz, 1H), 2.62 (broad s, 1H). LC-MS (method B): t_r = 0.80 min; $[M+H]^+$: 495.06.

(*R*)-*N*-(4-Bromophenyl)-5-(2-hydroxyethyl)-5-(4-methoxyphenyl)-3-(pyridin-3-yl)-4,5-dihydro-1H-pyrazole-1-carboxamide ((*R*)-11h) and (*S*)-*N*-(4-bromophenyl)-5-(2-hydroxyethyl)-5-(4-methoxyphenyl)-3-(pyridin-3-yl)-4,5-dihydro-1H-pyrazole-1-carboxamide ((*S*)-11h). Compounds **11h** was separated by HPLC using a chiral stationary phase (Diacel ChiralPak IB 5 μm column, 30 x 250 mm, EtOH / heptane 4:6 with 0.05% Et_2NH, 34 ml/min, 12 min). Compound **(*R*)-11h** eluted at 6.49 min, compound **(*S*)-11h** at 8.27 min. ^{1}H-NMR and LC-MS spectra for each compound was identical to **11h**. Enantiomeric purity > 95% by analytical HPLC (Diacel ChiralPak IS 5 μm column, 4.6 x 250 mm, EtOH / heptane 4:6 with 0.05% Et_2NH, 0.8 ml/min, 15 min). $[\alpha]_D$ (c = 1, methanol): -10.3 ° for **(*R*)-11h**, and +11.3 ° for **(*S*)-11h**.

X-ray structure analysis of (*S*)-11h. Formula: $C_{24}H_{23}BrN_4O_3$, formula weight 495.4, space group: P21212. The structure was deposited with Cambridge Crystallographic Data Centre, code 1498622.

***N*-(4-Fluorophenyl)-5-(methoxymethyl)-3-phenyl-5-(p-tolyl)-4,5-dihydro-1H-pyrazole-1-carboxamide (11i).** Obtained from a solution of the corresponding hydroxymethyl derivative (80 mg, 0.20 mmol) in THF (3 ml) at rt. NaH (60% in oil, 12 mg, 0.30 mmol) was added, and the mixture was stirred for 15 min. MeI (14 mg, 0.10 mmol) was added, and the mixture was stirred at 60 °C for 1 h. The mixture was diluted with water (30 ml), and was extracted ethyl acetate (50 ml). Purification by flash chromatography (ethyl acetate / hexanes 0:100 → 20:80) yielded the

desired product. ^{1}H NMR (500 MHz, $CDCl_3$) δ 8.25 (s, 1H), 7.73-7.76 (m, 2H), 7.47 (dd, J_1 = 9.1 Hz, J_2 = 4.8 Hz, 2H), 7.43-7.46 (m, 3H), 7.24 (d, J = 8.30 Hz, 2H), 7.16 (d, J = 8.00 Hz, 2H), 6.99 (t, J = 8.60 Hz, 2H), 4.45 (d, J = 9.2 Hz, 1H), 4.23 (d, J = 9.2 Hz, 1H), 3.98 (d, J = 17.6 Hz, 1H), 3.50 (s, 3H), 3.40 (d, J = 17.5 Hz, 1H), 2.33 (s, 3H). LC-MS (method B): t_r = 1.03 min; $[M+H]^+$: 418.05.

***N*-(4-Fluorophenyl)-5-(2-morpholinoethyl)-3-phenyl-5-(p-tolyl)-4,5-dihydro-1H-pyrazole-1-carboxamide (11j).** Obtained from the corresponding hydroxyethyl derivative (1.00 eq.) that was dissolved in DMSO/CH_2Cl_2 (1:4, 10 mL/mmol) at rt. *N*-(3-Dimethylaminopropyl)-*N*′-ethylcarbodiimide hydrochloride (6 eq.) and dichloroacetic acid (0.5 eq.) were added after each other. The reaction mixture was stirred at rt for 45 min. CH_2Cl_2 was added, and the mixture was washed with aq. sat. $NaHCO_3$. The organic layer was dried over $MgSO_4$, filtered, and the solvents were removed under reduced pressure to yield the crude aldehyde, which was converted to the desired, final product by reductive amination (1.3 eq. of the amine, 4.0 eq. of $BH(OAc)_3$, in THF at rt overnight). ^{1}H NMR (500 MHz, $CDCl_3$) δ 8.25 (s, 1H), 7.70-7.74 (m, 2H), 7.44-7.48 (m, 5H), 7.24 (d, J = 8.05 Hz, 2H), 7.17 (d, J = 8.10 Hz, 2H), 7.01 (t, J = 8.65 Hz, 2H), 3.53-3.96 (m, 4H), 3.47 (d = 17.5 Hz, 1H), 3.02-3.21 (broad s, 1H), 2.37-2.83 (m, 4H), 2.33 (s, 3H). LC-MS (method B): t_r = 0.84 min; $[M+H]^+$: 487.14.

5-(2-(Dimethylamino)ethyl)-*N*-(4-fluorophenyl)-3-phenyl-5-(p-tolyl)-4,5-dihydro-1H-pyrazole-1-carboxamide (11k). Obtained from the corresponding hydroxyethyl derivative similarly to compound **11j**. ^{1}H NMR (500 MHz, $CDCl_3$) δ 8.29 (s, 1H), 7.68-7.77 (m, 2H), 7.48 (dd, J_1 = 9.1 Hz, J_2 = 4.8 Hz, 2H), 7.44-7.47 (m, 3H), 7.23 (d, J = 8.30 Hz, 2H), 7.17 (d, J = 8.15 Hz, 2H), 7.01 (t, J = 8.60 Hz, 2H), 3.84 (d, J = 18.0 Hz, 1H), 3.47 (d, J = 18.05 Hz, 1H),

3.10-3.21 (m, 1H), 2.50-2.85 (m, 3H), 2.45 (broad s, 6H), 2.33 (s, 3H). LC-MS (method B): t_r = 0.83 min; $[M+H]^+$: 445.16.

***N*-(4-Fluorophenyl)-5-(2-(4-methylpiperazin-1-yl)ethyl)-3-phenyl-5-(p-tolyl)-4,5-dihydro-1H-pyrazole-1-carboxamide (11l).** Obtained from the corresponding hydroxyethyl derivative similarly to compound **11j**. ^{1}H NMR (500 MHz, $CDCl_3$) δ 8.24 (s, 1H), 7.70-7.74 (m, 2H), 7.44-7.51 (m, 5H), 7.25 (d, *J* = 8.30 Hz, 2H), 7.16 (d, *J* = 8.05 Hz, 2H), 7.00 (t, *J* = 8.60 Hz, 2H), 3.74-3.78 (m, 1H), 3.44 (d, *J* = 17.9 Hz, 1H), 3.02-3.16 (m, 1H), 2.40-3.01 (m, 11H), 2.32 (s, 3H), 2.30 (broad s, 3H). LC-MS (method B): t_r = 0.77 min; $[M+H]^+$: 500.17.

Biology

In vitro Methods – Measurement of calcium channel flux by means of FLIPR assays: HEK293 cells recombinantly expressing either voltage-dependent T-type calcium channel subunit alpha-1H ($Ca_v3.2$) or voltage-dependent L-type calcium channel subunit alpha-1C ($Ca_v1.2$) were assayed for calcium flux using the calcium indicator dye Fluo-4-AM (Molecular Devices) and FLIPR technology (Fluorometric Imaging Plate Reader, Molecular Devices) (Xie X, Van Deusen AL, Vitko I, Babu DA, Davies LA, Huynh N, Cheng H, Yang N, Barrett PQ, Perez-Reyes E. Validation of high throughput screening assays against three subtypes of Ca(v)3 T-type channels using molecular and pharmacologic approaches. Assay and Drug Development Technologies 2007, 5(2), 191-203). The HEK293 cells recombinantly expressing $Ca_v3.2$ were maintained in DMEM growth medium (Life Technologies) supplemented with 10 % Fetal Bovine Serum (FBS), 100 U/ml penicilin (Life Technologies), 100 μg/ml streptomycin (Life Technologies) and 1 mg/ml G418 (Life Technologies). HEK293 cells recombinantly expressing $Ca_v1.2$ were maintained in DMEM growth medium (Life Technologies) supplemented with 10

% FBS, 0.1 mg/ml G418 (Life Technologies), 0.1 mg/ml hygromycin (Life Technologies) and 40 μg/ml zeocin (Life Technologies).

Cells were washed once with PBS, then dissociated in 0.25 % trypsin/EDTA (Life Technologies) and seeded into poly-D-lysine coated 384-well black, clear bottom plates (BD Biosciences) at a density of 30,000 cells/well. The seeded plates were incubated overnight at 37°C.

Immediately prior to performing the assay, medium was removed and cells were treated for 1 hour at 37˚C with loading buffer containing HBSS 1X (137 mM NaCl; 5.4 mM KCl; 0.25 mM Na_2HPO_4; 1.3 mM $CaCl_2$; 0.4 mM $MgSO_4$; 0.5 mM $MgCl_2$; 0.4 mM KH_2PO_4, pH 7.4), 0.375 g/L $NaHCO_3$, 20 mM Hepes, supplemented with 3 μM Fluo-4-AM and 0.15 % Pluronic (Life Technologies). The cells are then washed three times with assay buffer (HBSS 1X; 0.375 g/L $NaHCO_3$; 20 mM Hepes; 1 % FBS; pH 7.4) and allowed to rest in 50 μl of wash buffer for 30 minutes.

Stock solutions of test compounds were prepared to a concentration of 10 mM in DMSO. For the Cav3.2 assay, serial dilutions of the compounds were prepared in TEAC buffer (100 mM tetraethylammonium chloride; 20 mM Hepes; 2.5 mM $CaCl_2$; 5 mM KCl; 1 mM $MgCl_2$; 1 % FBS; pH 7.2), for the $Ca_v1.2$ assay serial dilutions were prepared in assay buffer. Test compounds were added to the cells to give a 3-fold dilution series ranging from 10 μM to 0.05 nM. The compounds were incubated with the cells for 3 minutes and Ca^{2+} entry was stimulated by adding either $CaCl_2$ to a final concentration of 10 mM ($Ca_v3.2$ assay) or by adding KCl to a final concentration of 20 mM ($Ca_v1.2$ assay). The kinetics of fluorescence increase were recorded for every well and the area under the fluorescence trace for every compound concentration was used to generate inhibition curves using non-linear regression sigmoidal

concentration-response curve analysis with in-house software. IC50 values were calculated and represent the compound concentration required to inhibit 50% of the signal that is obtained in the presence of vehicle instead of test compound. In analogy, antagonistic activities (IC50 values) of all exemplified compounds have been measured for the $Ca_v3.1$- and the $Ca_v3.3$-channel. Antagonistic activities (IC50 values) of all exemplified compounds are in the range of 0.3 to 1210 nM with respect to $Ca_v3.1$; and in the range of 0.8 to 1280 nM with respect to $Ca_v3.3$.

Electrophysiology: *Patch-clamp assays.* Compounds were evaluated for block of hCav3.1, hCav3.2, and hCav3.3 channels using CHO cells stably expressing the human Cacna1h, Cacna1g, and Cacna1i genes (from E. Perez-Reyes, U. Virginia, USA) and the QPatch platform (Sophion, Ballerup, Denmark). Ca^{2+} tail currents were measured at -60 mV following a 3-ms depolarization to +20 mV from holding voltages of either -90 mV or -60 mV. The Cs-Glutamate-based internal solution also contained 1 mM TBA, 25 mM Cl-, 1.8 mM Ca^{2+}, 1 mM Mg^{2+}, 11 mM BAPTA and 20 mM HEPES. The TEA-Cl-based external solution also contained 5 mM Ca^{2+}, 0.5 mM Mg^{2+} and 10 mM HEPES. Compound effects were quantified 150s after application to the cells. Compounds were evaluated for block of neuronal Na and K channels using rat cortical neurons (cryopreserved or freshly-prepared) dissociated from E18 Wistar rat embryos and cultured for 9 to 15 days, using a manual patch-clamp system (HEKA-10 amplifier, Darmstadt, Germany). Fast and slow K^+ currents were measured during one 50-ms depolarization to 0 mV from a holding potential of -80 mV, as the peak outward current and as the outward current at the end-of-pulse. Na^+ currents were measured during a 30 Hz train of fifteen 10-ms depolarizations to 0 mV at 50 Hz from a holding potential of -80 mV, and compound effects were measured as effect on the peak inward current during the first and last pulses of the train. The K-Cl-based internal solution also contained 10 mM Na^+, 11 mM Mg^{2+}, 5

mM EGTA, 0.1 mM GTP, 5 mM ATP and 10 mM HEPES. The Na-Cl-based external solution also contained 4 mM K^+, 1.2 mM Ca^{2+}, 1 mM Mg^{2+} and 10 mM HEPES. Compound effects were quantified at least180s after application to the cells. *hKV11.1 ("hERG") assay.* Compounds were evaluated for block of hKV11.1 channels using CHO cells stably expressing the hERG gene (bSys, Witterswil, Switzerland) and the QPatch platform (Sophion, Ballerup, Denmark). K+ tail currents were measured at -40 mV following a 500-ms depolarization to +20 mV from a holding voltage of -80 mV. The external solution contained 150 mM Na+, 4 mM K+, 1 mM Mg2+ and 1.2 mM Ca2+. Compound effects were quantified 3 minutes after application to the cells.

Pharmacology: Male Wistar rats and WAG/Rij rats were purchased from Harlan (Horst Netherlands) and Charles River (Sulzfeld, Germany) respectively. All animals were maintained under standard lab conditions (temperature 20 ± 2°C, relative humidity 55–70%, on a 12 h light / 12 h dark cycle from 6 am to 6 pm) with free access to normal chow and water. The experimental procedures used in this study were approved based on international guidelines and adherence to Swiss federal regulations on animal experimentation (license # KV-BL 420 for kindling experiment, # KV-BL 205 for EEG experiments).

Amygdala-kindling rat model: Adult male Wistar rats (Harlan Laboratories, Netherlands; body weight 300-350g) were stereotaxically implanted with twisted bipolar plastic-coated stainless steel electrode (MS333-2-BIU 10mm, Plastics One, Roanoke, USA) into the right basolateral amygdala under isoflurane anesthesia. To place the electrode, trepanations were made in the skull and the electrode was lowered into the right basolateral amygdala (from bregma: anterior-posterior (AP): -2.5mm, medio-lateral (ML): -3.5mm, dorso-ventral (DV): -8.6mm; α=10°) and secured to the skull with screws and dental acrylate. After one week of recovery, they were handled daily and habituated over one week to the kindling set-up.

Kindling procedure: For a kindling session each rat was placed individually into a smooth acrylic plastic, round-bottomed bowl (Ø 36cm, height 36cm, BASi movement-responsive caging system; West Lafayette, USA) and its intracranial implanted electrode was connected to the stimulator (STG4008, Multichannel Systems GmbH, Germany) and the recording devices (PowerLab 8/35, ADInstruments Ltd, Oxford, UK) via a cable (335-340/3 (C), Plastics One, Roanoke, USA). Before starting the daily electrical stimulation, the pre-kindling afterdischarge threshold (ADT) was defined by administering a series of electrical stimulations (1s-train of 50 Hz square-wave biphasic pulses of 1-ms duration) at 1-min intervals with ascending intensity, starting at 10μA and increasing in 10μA-steps. The ADT was defined as the minimal stimulation intensity necessary to evoke an afterdischarge (electroencephalographically measured neuronal hyper-synchronous activity with an amplitude 2-times higher than baseline amplitude and a frequency of $\geq$1 Hz) of at least 3sec duration. For the kindling procedure, each rat was exposed once daily to an electrical stimulation and the behavioral symptoms of the evoked seizure were observed and classified according to the modified Racine scale (stage 0, arrest, wet dog shakes, normal behaviour; stage 1, facial twitches: nose, lips, eyes; stage 2, chewing, head nodding; stage 3, forelimb clonus; stage 4, rearing, falling on forelimbs; stage 5, rearing, falling on side or back, rolling). The electrical stimulus consists of a 1s-train of 50 Hz square-wave biphasic pulses of 1-ms duration at an intensity of 400μA (suprathreshold intensity). The stimulus was applied daily until each rat was fully kindled, i.e. it showed seizures of severity stage 4 and 5 upon electrical stimulation in at least ten consecutive kindling sessions. Finally, the post-kindling ADT was defined using the same protocol as described for the pre-kindling ADT. Due to the kindling-induced increase in seizure susceptibility of the temporal lobe tissue the post-kindling ADT is lower than the pre-kindling ADT.

Data Scoring and analysis. The duration of electroencephalographic seizures (afterdischarge duration, ADD) was recorded using LabChart7 Pro software (ADInstruments Ltd, Oxford, UK). Simultaneously, videos were recorded to evaluate seizure stage (SS) and duration of convulsions of seizure stage 3-5 (SD). Videos were saved together with the EEG data.

Drug testing: Acute drug effects were evaluated in groups of 6 fully kindled rats in a randomized cross-over design with 48h between drug and vehicle applications. Following oral administration of drug or vehicle, drug testing included ADT determination and monitoring electroencephalographic (ADD) and behavioral (SS, SD) correlates of the evoked seizure at ADT by a experimenter blind to treatment assignment.

WAG/Rij rat model: Surgery: Adult male WAG/Rij rats (aged at least 6 months, body weight 300-350g) were equipped with the TL11M2-F20-EET implant (Data Science International, St Paul, MN, USA) that consists of 4 leads (2 pairs) for EEG and electromyographic (EMG) measurements by telemetry. For surgery, rats were anesthetized with isoflurane and placed in a stereotaxic apparatus. The transmitter's body was placed subcutaneously along the dorsal flank of the rat and EEG and EMG leads were routed subcutaneously to an incision accessing the cranium. Trepanations were made in the skull and EEG electrodes were placed on the surface of the cortex (from bregma: 1st electrode: AP: -1mm, ML: -2.5mm, DV: 0mm; 2nd electrode: AP: + mm, ML: -3.5mm, DV: 0mm) and secured to the skull with screws and dental acrylate. The EMG leads were placed in either side of cervical muscles and sutured in place. After one week of recovery, rats could be included in pharmacology studies.

Procedure. The entire telemetry system originates from Data Sciences International (USA). It comprises transmitters, receiver plates (PhysioTel RPC-1), data exchange matrixes (1 for 4

receivers) and computers installed with the Dataquest A.R.T. 4.1 Gold software for data acquisition (1 computer for 8 receivers). For continuous EEG/EMG recordings, single-housed implanted rats, in their home cage, were placed on the receiver plate within a sound attenuating scantainer that is equipped with light and fan to ensure a quiet environment. EEG seizures were evaluated using Neuroscore 2.0 or 2.1 software (Data Science International, St Paul, MN, USA).

Drug testing. Acute drug effects on spontaneous seizures were evaluated in groups of 6-8 rats in a randomized cross-over design with at least 72hrs between drug and vehicle applications. Following a 24-hrs baseline recording, drug or vehicle was administered 30 minutes before beginning of the dark phase and number and duration of EEG seizures were assessed.

Telemetric Cardiovascular Safety Studies: (Brockway, B. P.; Mills, P. A.; Azar, S. H. A New Method for Continuous Chronic Measurement and Recording of Blood Pressure, Heart Rate and Activity in the Rat via Radio-Telemetry. Clin. and Exper. Hyper. -Theory and Practice 1991, A13, 885-895; Guiol, C.; Ledoussal, C.; Surgé, J.-M. A Radiotelemetry System for Chronic Measurement of Blood Pressure and Heart Rate in the Unrestrained Rat Validation of the Method. J. Pharmcol. Toxicol. Methods 1992, 28, 99-105). The effect of compound 6c on mean arterial pressure (MAP), heart rate (HR) and electrocardiogram was assessed by single oral administration (5 ml/kg) as a suspension in methylcellulose (0.5% w/v) in water to male spontaneously hypertensive rats (SHRs) equipped with a telemetric system recording mean arterial blood pressure and electrocardiogram. Compound administration took place in the morning, i.e. during the sleep phase of the animals.

Solubility: For each compound 40 mL of a 10 mM DMSO stock solution were dispensed using a multi-channel pipette (20-300µL, Research Pro, Eppendorf) into a 96-well microplate (PP, F-

bottom Chimney Well ref: 655201, Greiner bio-one) and the solvent was evaporated under reduced pressure in a Combidancer (Hettich AG). Each well was filled with 200 mL of the corresponding buffer solution : water, HCl 0.1 M, citrate buffer (55 mM) pH=4.0, phosphate buffer (67 mM) pH=7.0, TRIS buffer (50 mM) pH=9.0, NaOH 0.1 M. The plate was stirred for 24h at 300 rpm on a Vibramax 100 (Heidolph) at room temperature. The resulting biphasic systems were withdrawn with a laboratory automated work station Biomek FXP (Beckman Coulter) and put into a 96-well filter plate (300µL, PVDF, 0.45µm SHT, 50/CS ref: 200995-100, Screening Devices). During centrifugation (3'000rpm, 2min, 5810R Eppendorf), the filtrates were collected into a 96-well plate (0.2mL, non-skirted, PCR plate ref : AB-0600, Thermo Scientific). Solubilities were determined by measuring the concentrations of these solutions using a modular Shimadzu HPLC system with UV detection and comparing with the results of calibrated solutions.

ASSOCIATED CONTENT

Supporting Information. Experimental details and NMR spectra are available as supporting information. This material is available free of charge via the Internet at http://pubs.acs.org.

AUTHOR INFORMATION

Corresponding Author

* Olivier Bezençon, Actelion Pharmaceuticals Ltd, Gewerbestrasse 16, CH - 4123 Allschwil. Phone + 41 61 565 65 77. Email Olivier.bezencon@actelion.com

Present Addresses

†Dennis Downing: General Motors, 2100 Burlingame Ave. SW, Grand Rapids, MI 49509. Johannes Mosbacher: F. Hoffmann-La Roche Ltd., CH-Basel. Thomas Pfeifer: ADME & more, Märktweg 30, D-79576 Weil am Rhein, Germany.

Author Contributions

The manuscript was written through contributions of all authors. All authors have given approval to the final version of the manuscript.

ACKNOWLEDGMENT

We would like to thank the following persons for their invaluable contribution to the work presented here: Martin Faes, Sophie Moujon, Sven Glutz, Claire Hinder, Ann Nathalie de Leon, Dominic Juchli, Christine Berthion, Jean-Marie Pilven, Daniel Bur, Celia Mueller Grandjean, Alexandre Peter, Jacques Mawet, Daniel Wanner, Céline Bortolamiol, Alexander Hasler.

ABBREVIATIONS

ABT: 1-aminobenzotriazole; AED: antiepileptic drug; AMPA: α-amino-3-hydroxy-5-methyl-4-isoxazolepropionic acid receptor; BCRP: breast cancer resistant protein; BuLi: *n*-butyl lithium; ECG: electrocardiogram; EEG: electroencephalogram; Et: ethyl; Fassif: fasted state simulating instestinal fluid; Fessif: fed state simulating instestinal fluid; FLIPR: fluorometric imaging plate reader; IGE: idiopathic generalized epilepsy; GABA: γ-aminobutyric acid; GAERS: genetic absence epilepsy in rats from Strasbourg; HTS: high-throughput screening; LE: ligand

efficiency: LLE: lipophilic ligand efficiency; MCPBA: *meta*-chloroperbenzoic acid; MDR1: multidrug resistance protein; MPO: multiple parameter optimization; Pgp: P-glycoprotein; PSA: polar surface area; PTSA: *para*-toluenesulfonic acid; rt: room temperature; t_R: retention time; TTCC: T-Type calcium channel; WAG/Rij rat: Wistar albino rats of Glaxo Rijswijk.

REFERENCES

1. http://www.who.int/mediacentre/factsheets/fs999/en/

2. (a) Berg, A. T.; Scheffer, I. E. New concepts in classification of the epilepsies: entering the 21st century. *Epilepsia* **2011,** *52*, 1058-1062; (b) Berg, A. T.; Berkovic, S. F.; Brodie, M. J.; Buchhalter, J.; Cross, J. H.; van Emde Boas, W.; Engel, J.; French, J.; Glauser, T. A.; Mathern, G. W.; Moshe, S. L.; Nordli, D.; Plouin, P.; Scheffer, I. E. Revised terminology and concepts for organization of seizures and epilepsies: report of the ILAE Commission on Classification and Terminology, 2005-2009. *Epilepsia* **2010,** *51*, 676-685.

3. Willow, M.; Gonoi, T.; Catterall, W. A. Voltage clamp analysis of the inhibitory actions of diphenylhydantoin and carbamazepine on voltage-sensitive sodium channels in neuroblastoma cells. *Mol. Pharmacol.* **1985,** *27*, 549-558.

4. (a) Beydoun, A.; D'Souza, J.; Hebert, D.; Doty, P. Lacosamide: pharmacology, mechanisms of action and pooled efficacy and safety data in partial-onset seizures. *Expert Rev. Neurother.* **2009,** *9*, 33-42; (b) Curia, G.; Biagini, G.; Perucca, E.; Avoli, M. Lacosamide: a new approach to target voltage-gated sodium currents in epileptic disorders. *CNS Drugs* **2009,** *23*, 555-568; (c) Huang, C. W.; Hung, T. Y.; Wu, S. N. The inhibitory actions by lacosamide, a functionalized amino acid, on voltage-gated Na+ currents. *Neuroscience* **2015,** *287*, 125-136; (d)

Nakatani, Y.; Masuko, H.; Amano, T. Effect of lamotrigine on Na(v)1.4 voltage-gated sodium channels. *J. Pharmacol. Sci.* **2013,** *123*, 203-206; (e) Niespodziany, I.; Leclere, N.; Vandenplas, C.; Foerch, P.; Wolff, C. Comparative study of lacosamide and classical sodium channel blocking antiepileptic drugs on sodium channel slow inactivation. *J. Neurosci. Res.* **2013,** *91*, 436-443.

5. (a) Liu, G.; Yarov-Yarovoy, V.; Nobbs, M.; Clare, J. J.; Scheuer, T.; Catterall, W. A. Differential interactions of lamotrigine and related drugs with transmembrane segment IVS6 of voltage-gated sodium channels. *Neuropharmacology* **2003,** *44*, 413-422; (b) Kuo, C. C.; Lu, L. Characterization of lamotrigine inhibition of Na+ channels in rat hippocampal neurones. *Br. J. Pharmacol.* **1997,** *121*, 1231-8; (c) Xie, X.; Lancaster, B.; Peakman, T.; Garthwaite, J. Interaction of the antiepileptic drug lamotrigine with recombinant rat brain type IIA Na+ channels and with native Na+ channels in rat hippocampal neurones. *Pfluegers Arch.* **1995,** *430*, 437-446.

6. Holder, J. L., Jr.; Wilfong, A. A. Zonisamide in the treatment of epilepsy. *Expert Opin. Pharmacother.* **2011,** *12*, 2573-2581.

7. (a) Gunthorpe, M. J.; Large, C. H.; Sankar, R. The mechanism of action of retigabine (ezogabine), a first-in-class K+ channel opener for the treatment of epilepsy. *Epilepsia* **2012,** *53*, 412-424; (b) Main, M. J.; Cryan, J. E.; Dupere, J. R.; Cox, B.; Clare, J. J.; Burbidge, S. A. Modulation of KCNQ2/3 potassium channels by the novel anticonvulsant retigabine. *Mol. Pharmacol.* **2000,** *58*, 253-262.

8. Dibue, M.; Kamp, M. A.; Alpdogan, S.; Tevoufouet, E. E.; Neiss, W. F.; Hescheler, J.; Schneider, T. Cav 2.3 (R-type) calcium channels are critical for mediating anticonvulsive and neuroprotective properties of lamotrigine in vivo. *Epilepsia* **2013,** *54*, 1542-1550.

9. Crepeau, A. Z.; Treiman, D. M. Levetiracetam: a comprehensive review. *Expert Rev. Neurother.* **2010,** *10*, 159-171.

10. White, H. S. Molecular pharmacology of topiramate: managing seizures and preventing migraine. *Headache* **2005,** *45 Suppl 1*, S48-S56.

11. (a) Zaccara, G.; Giovannelli, F.; Cincotta, M.; Iudice, A. AMPA receptor inhibitors for the treatment of epilepsy: the role of perampanel. *Expert Rev. Neurother.* **2013,** *13*, 647-655; (b) Krauss, G. L.; Perucca, E.; Ben-Menachem, E.; Kwan, P.; Shih, J. J.; Squillacote, D.; Yang, H.; Gee, M.; Zhu, J.; Laurenza, A. Perampanel, a selective, noncompetitive alpha-amino-3-hydroxy-5-methyl-4-isoxazolepropionic acid receptor antagonist, as adjunctive therapy for refractory partial-onset seizures: interim results from phase III, extension study 307. *Epilepsia* **2013,** *54*, 126-134; (c) French, J. A.; Krauss, G. L.; Steinhoff, B. J.; Squillacote, D.; Yang, H.; Kumar, D.; Laurenza, A. Evaluation of adjunctive perampanel in patients with refractory partial-onset seizures: results of randomized global phase III study 305. *Epilepsia* **2013,** *54*, 117-125; (d) Hanada, T.; Hashizume, Y.; Tokuhara, N.; Takenaka, O.; Kohmura, N.; Ogasawara, A.; Hatakeyama, S.; Ohgoh, M.; Ueno, M.; Nishizawa, Y. Perampanel: a novel, orally active, noncompetitive AMPA-receptor antagonist that reduces seizure activity in rodent models of epilepsy. *Epilepsia* **2011,** *52*, 1331-1340.

12. Kwan, P.; Arzimanoglou, A.; Berg, A. T.; Brodie, M. J.; Allen Hauser, W.; Mathern, G.; Moshe, S. L.; Perucca, E.; Wiebe, S.; French, J. Definition of drug resistant epilepsy: consensus

proposal by the ad hoc Task Force of the ILAE Commission on Therapeutic Strategies. *Epilepsia* **2010,** *51*, 1069-1077.

13. (a) Loscher, W.; Klitgaard, H.; Twyman, R. E.; Schmidt, D. New avenues for anti-epileptic drug discovery and development. *Nat. Rev. Drug Discovery* **2013,** *12*, 757-776; (b) Loscher, W.; Schmidt, D. Modern antiepileptic drug development has failed to deliver: ways out of the current dilemma. *Epilepsia* **2011,** *52*, 657-678; (c) Schmidt, D.; Sillanpaa, M. Evidence-based review on the natural history of the epilepsies. *Curr. Opin. Neurol.* **2012,** *25*, 159-163.

14. (a) Lee, J. H.; Daud, A. N.; Cribbs, L. L.; Lacerda, A. E.; Pereverzev, A.; Klockner, U.; Schneider, T.; Perez-Reyes, E. Cloning and expression of a novel member of the low voltage-activated T-type calcium channel family. *J. Neurosci.* **1999,** *19*, 1912-1921; (b) Perez-Reyes, E. Molecular physiology of low-voltage-activated t-type calcium channels. *Physiol. Rev.* **2003,** *83*, 117-161.

15. Talley, E. M.; Cribbs, L. L.; Lee, J. H.; Daud, A.; Perez-Reyes, E.; Bayliss, D. A. Differential distribution of three members of a gene family encoding low voltage-activated (T-type) calcium channels. *J. Neurosci.* **1999,** *19*, 1895-1911.

16. (a) Shin, H. S. T-type Ca2+ channels and absence epilepsy. *Cell Calcium* **2006,** *40*, 191-196; (b) Cheong, E.; Shin, H. S. T-type Ca(2+) channels in absence epilepsy. *Pfluegers Arch.* **2014,** *466*, 719-734; (c) Khosravani, H.; Zamponi, G. W. Voltage-gated calcium channels and idiopathic generalized epilepsies. *Physiol. Rev.* **2006,** *86*, 941-966; (d) Zamponi, G. W.; Lory, P.; Perez-Reyes, E. Role of voltage-gated calcium channels in epilepsy. *Pfluegers Arch.* **2010,** *460*, 395-403.

17. Glauser, T. A.; Cnaan, A.; Shinnar, S.; Hirtz, D. G.; Dlugos, D.; Masur, D.; Clark, P. O.; Capparelli, E. V.; Adamson, P. C. Ethosuximide, valproic acid, and lamotrigine in childhood absence epilepsy. *N. Engl. J. Med.* **2010,** *362*, 790-809.

18. Goren, M. Z.; Onat, F. Ethosuximide: from bench to bedside. *CNS Drug Rev.* **2007,** *13*, 224-239.

19. (a) Chen, Y.; Lu, J.; Pan, H.; Zhang, Y.; Wu, H.; Xu, K.; Liu, X.; Jiang, Y.; Bao, X.; Yao, Z.; Ding, K.; Lo, W. H.; Qiang, B.; Chan, P.; Shen, Y.; Wu, X. Association between genetic variation of CACNA1H and childhood absence epilepsy. *Ann. Neurol.* **2003,** *54*, 239-243; (b) Khosravani, H.; Altier, C.; Simms, B.; Hamming, K. S.; Snutch, T. P.; Mezeyova, J.; McRory, J. E.; Zamponi, G. W. Gating effects of mutations in the Cav3.2 T-type calcium channel associated with childhood absence epilepsy. *J. Biol. Chem.* **2004,** *279*, 9681-9684; (c) Vitko, I.; Chen, Y.; Arias, J. M.; Shen, Y.; Wu, X. R.; Perez-Reyes, E. Functional characterization and neuronal modeling of the effects of childhood absence epilepsy variants of CACNA1H, a T-type calcium channel. *J. Neurosci.* **2005,** *25*, 4844-4855.

20. (a) Eckle, V. S.; Shcheglovitov, A.; Vitko, I.; Dey, D.; Yap, C. C.; Winckler, B.; Perez-Reyes, E. Mechanisms by which a CACNA1H mutation in epilepsy patients increases seizure susceptibility. *J. Physiol.* **2014,** *592*, 795-809; (b) Heron, S. E.; Khosravani, H.; Varela, D.; Bladen, C.; Williams, T. C.; Newman, M. R.; Scheffer, I. E.; Berkovic, S. F.; Mulley, J. C.; Zamponi G. W., Extended spectrum of idiopathic generalized epilepsies associated with CACNA1H functional variants. *Ann. Neurol.* **2007,** *62*, 560-568.

21. Kim, D.; Song, I.; Keum, S.; Lee, T.; Jeong, M. J.; Kim, S. S.; McEnery, M. W.; Shin, H. S. Lack of the burst firing of thalamocortical relay neurons and resistance to absence seizures in mice lacking alpha(1G) T-type Ca(2+) channels. *Neuron* **2001,** *31*, 35-45.

22. Yang, Z. Q.; Barrow, J. C.; Shipe, W. D.; Schlegel, K. A.; Shu, Y.; Yang, F. V.; Lindsley, C. W.; Rittle, K. E.; Bock, M. G.; Hartman, G. D.; Uebele, V. N.; Nuss, C. E.; Fox, S. V.; Kraus, R. L.; Doran, S. M.; Connolly, T. M.; Tang, C.; Ballard, J. E.; Kuo, Y.; Adarayan, E. D.; Prueksaritanont, T.; Zrada, M. M.; Marino, M. J.; Graufelds, V. K.; DiLella, A. G.; Reynolds, I. J.; Vargas, H. M.; Bunting, P. B.; Woltmann, R. F.; Magee, M. M.; Koblan, K. S.; Renger, J. J. Discovery of 1,4-substituted piperidines as potent and selective inhibitors of T-type calcium channels. *J. Med. Chem.* **2008,** *51*, 6471-6477.

23. Tringham, E.; Powell, K. L.; Cain, S. M.; Kuplast, K.; Mezeyova, J.; Weerapura, M.; Eduljee, C.; Jiang, X.; Smith, P.; Morrison, J. L.; Jones, N. C.; Braine, E.; Rind, G.; Fee-Maki, M.; Parker, D.; Pajouhesh, H.; Parmar, M.; O'Brien, T. J.; Snutch, T. P. T-type calcium channel blockers that attenuate thalamic burst firing and suppress absence seizures. *Sci. Transl. Med.* **2012,** *4*, 1-13.

24. (a) Hosford, D. A. Models of primary generalized epilepsy. *Curr. Opin. Neurol.* **1995,** *8*, 121-125; (b) Coenen, A. M.; Drinkenburg, W. H.; Inoue, M.; van Luijtelaar, E. L. Genetic models of absence epilepsy, with emphasis on the WAG/Rij strain of rats. *Epilepsy Res.* **1992,** *12*, 75-86.

25. Becker, A. J.; Pitsch, J.; Sochivko, D.; Opitz, T.; Staniek, M.; Chen, C. C.; Campbell, K. P.; Schoch, S.; Yaari, Y.; Beck, H. Transcriptional upregulation of Cav3.2 mediates epileptogenesis in the pilocarpine model of epilepsy. *J. Neurosci.* **2008,** *28*, 13341-13353.

26. Matar, N.; Jin, W.; Wrubel, H.; Hescheler, J.; Schneider, T.; Weiergraber, M. Zonisamide block of cloned human T-type voltage-gated calcium channels. *Epilepsy Res.* **2009,** *83*, 224-234.

27. Egan, M. F.; Zhao, X.; Smith, A.; Troyer, M. D.; Uebele, V. N.; Pidkorytov, V.; Cox, K.; Murphy, M.; Snavely, D.; Lines, C.; Michelson, D. Randomized controlled study of the T-type calcium channel antagonist MK-8998 for the treatment of acute psychosis in patients with schizophrenia. *Hum. Psychopharmacol.* **2013,** *28*, 124-133.

28. Zamponi, G. W. Targeting voltage-gated calcium channels in neurological and psychiatric diseases. *Nat. Rev. Drug. Discovery* **2016,** *15*, 19-34.

29. (a) Choe, W.; Messinger, R. B.; Leach, E.; Eckle, V. S.; Obradovic, A.; Salajegheh, R.; Jevtovic-Todorovic, V.; Todorovic, S. M. TTA-P2 is a potent and selective blocker of T-type calcium channels in rat sensory neurons and a novel antinociceptive agent. *Mol. Pharmacol.* **2011,** *80*, 900-910; (b) Francois, A.; Kerckhove, N.; Meleine, M.; Alloui, A.; Barrere, C.; Gelot, A.; Uebele, V. N.; Renger, J. J.; Eschalier, A.; Ardid, D.; Bourinet, E. State-dependent properties of a new T-type calcium channel blocker enhance Ca(V)3.2 selectivity and support analgesic effects. *Pain* **2013,** *154*, 283-293.

30. (a) Miwa, H.; Kondo, T. T-type calcium channel as a new therapeutic target for tremor. *Cerebellum* **2011,** *10* (3), 563-569; (b) Handforth, A.; Homanics, G. E.; Covey, D. F.; Krishnan, K.; Lee, J. Y.; Sakimura, K.; Martin, F. C.; Quesada, A. T-type calcium channel antagonists suppress tremor in two mouse models of essential tremor. *Neuropharmacology* **2010,** *59*, 380-387.

31. Miwa, H.; Koh, J.; Kajimoto, Y.; Kondo, T. Effects of T-type calcium channel blockers on a parkinsonian tremor model in rats. *Pharmacol. Biochem. Behav.* **2011,** *97*, 656-659.

32. Uebele, V. N.; Gotter, A. L.; Nuss, C. E.; Kraus, R. L.; Doran, S. M.; Garson, S. L.; Reiss, D. R.; Li, Y.; Barrow, J. C.; Reger, T. S.; Yang, Z. Q.; Ballard, J. E.; Tang, C.; Metzger, J. M.; Wang, S. P.; Koblan, K. S.; Renger, J. J. Antagonism of T-type calcium channels inhibits high-fat diet-induced weight gain in mice. *J. Clin. Invest.* **2009,** *119*, 1659-1667.

33. Uslaner, J. M.; Vardigan, J. D.; Drott, J. M.; Uebele, V. N.; Renger, J. J.; Lee, A.; Li, Z.; Le, A. D.; Hutson, P. H. T-type calcium channel antagonism decreases motivation for nicotine and blocks nicotine- and cue-induced reinstatement for a response previously reinforced with nicotine. *Biol. Psychiatry* **2010,** *68*, 712-718.

34. Uslaner, J. M.; Smith, S. M.; Huszar, S. L.; Pachmerhiwala, R.; Hinchliffe, R. M.; Vardigan, J. D.; Nguyen, S. J.; Surles, N. O.; Yao, L.; Barrow, J. C.; Uebele, V. N.; Renger, J. J.; Clark, J.; Hutson, P. H. T-type calcium channel antagonism produces antipsychotic-like effects and reduces stimulant-induced glutamate release in the nucleus accumbens of rats. *Neuropharmacology* **2012,** *62*, 1413-1421.

35. Xie, X.; Van Deusen, A. L.; Vitko, I.; Babu, D. A.; Davies, L. A.; Huynh, N.; Cheng, H.; Yang, N.; Barrett, P. Q.; Perez-Reyes, E. Validation of high throughput screening assays against three subtypes of Ca(v)3 T-type channels using molecular and pharmacologic approaches. *Assay Drug Dev. Technol.* **2007,** *5*, 191-203.

36. Godfraind, T.; Ertel, E. *Calcium Channel Blockers*. Birkhäuser: Basel, 2004.

37. (a) Mishriky, N.; Asaad, F. M.; Ibrahim, Y. A.; Girgis, A. S. New 2-pyrazolines of anticipated molluscicidal activity. *Pharmazie* **1996,** *51*, 544-8; (b) Cox, C. D.; Breslin, M. J.; Mariano, B. J. two-step synthesis of β-alkyl chalcones and their use in the synthesis of 3,5-diaryl-5-alkyl-4,5-dihydropyrazoles. *Tetrahedron Lett.* **2004,** *45*, 1489-1493.

38. Ritchie, T. J.; Macdonald, S. J. Physicochemical descriptors of aromatic character and their use in drug discovery. *J. Med. Chem.* **2014**, *57*, 7206-7215.

39. Gleeson, M. P. Plasma protein binding affinity and its relationship to molecular structure: an in-silico analysis. *J. Med. Chem.* **2007,** *50*, 101-112.

40. Wager, T. T.; Hou, X.; Verhoest, P. R.; Villalobos, A. Moving beyond rules: the development of a central nervous system multiparameter optimization (CNS MPO) approach to enable alignment of druglike properties. *ACS Chem. Neurosci.* **2010,** *1*, 435-449.

41. Ertel, E. A.; Cohen, C. J. Voltage-dependent interactions: The influence and significance of membrane potential on drug-receptor interactions. *Drug Dev. Res.* **2004,** *33*, 203-213.

42. (a) Shipe, W. D.; Barrow, J. C.; Yang, Z. Q.; Lindsley, C. W.; Yang, F. V.; Schlegel, K. A.; Shu, Y.; Rittle, K. E.; Bock, M. G.; Hartman, G. D.; Tang, C.; Ballard, J. E.; Kuo, Y.; Adarayan, E. D.; Prueksaritanont, T.; Zrada, M. M.; Uebele, V. N.; Nuss, C. E.; Connolly, T. M.; Doran, S. M.; Fox, S. V.; Kraus, R. L.; Marino, M. J.; Graufelds, V. K.; Vargas, H. M.; Bunting, P. B.; Hasbun-Manning, M.; Evans, R. M.; Koblan, K. S.; Renger, J. J. Design, synthesis, and evaluation of a novel 4-aminomethyl-4-fluoropiperidine as a T-type Ca2+ channel antagonist. *J. Med. Chem.* **2008,** *51*, 3692-3695; (b) Schlegel, K. A.; Yang, Z. Q.; Reger, T. S.; Shu, Y.; Cube, R.; Rittle, K. E.; Bondiskey, P.; Bock, M. G.; Hartman, G. D.; Tang, C.; Ballard, J.; Kuo, Y.;

Prueksaritanont, T.; Nuss, C. E.; Doran, S. M.; Fox, S. V.; Garson, S. L.; Kraus, R. L.; Li, Y.; Uebele, V. N.; Renger, J. J.; Barrow, J. C. Discovery and expanded SAR of 4,4-disubstituted quinazolin-2-ones as potent T-type calcium channel antagonists. *Bioorg. Med. Chem. Lett.* **2010,** *20*, 5147-5152; (c) Yang, Z. Q.; Schlegel, K. A.; Shu, Y.; Reger, T. S.; Cube, R.; Mattern, C.; Coleman, P. J.; Small, J.; Hartman, G. D.; Ballard, J.; Tang, C.; Kuo, Y.; Prueksaritanont, T.; Nuss, C. E.; Doran, S.; Fox, S. V.; Garson, S. L.; Li, Y.; Kraus, R. L.; Uebele, V. N.; Taylor, A. B.; Zeng, W.; Fang, W.; Chavez-Eng, C.; Troyer, M. D.; Luk, J. A.; Laethem, T.; Cook, W. O.; Renger, J. J.; Barrow, J. C. Short-acting T-type calcium channel antagonists significantly modify sleep architecture in rodents. *ACS Med .Chem. Lett.* **2010,** *1*, 504-509.

43. (a) Racine, R. J. Modification of seizure activity by electrical stimulation. II. Motor seizure. *Electroencephalogr. Clin. Neurophysiol.* **1972,** *32*, 281-94; (b) Racine, R. J. Modification of seizure activity by electrical stimulation. I. After-discharge threshold. *Electroencephalogr. Clin. Neurophysiol.* **1972,** *32*, 269-279.

44. Casillas-Espinosa, P. M.; Hicks, A.; Jeffreys, A.; Snutch, T. P.; O'Brien, T. J.; Powell, K. L. Z944, a novel selective T-type calcium channel antagonist delays the progression of seizures in the amygdala kindling model. *PLoS One* **2015,** *10*, e0130012.

Table 1. Compounds 5a-m and potencies on $Ca_v3.2$ and $Ca_v1.2$

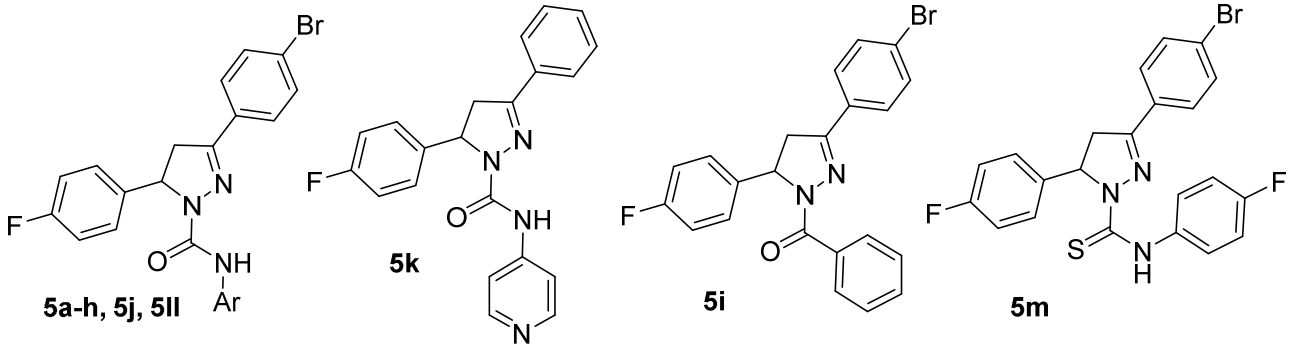

Compound	Ar	$Ca_v3.2$ IC_{50} (nM)[a]	$Ca_v1.2$ IC_{50} (nM)[a]
5a	Phenyl	68	>10000
5b	4-Fluorophenyl	16	>10000
5c	3-Fluorophenyl	46	>10000
5d	2-Fluorophenyl	>10000	>10000
5e	4-Methoxyphenyl	447	>10000
5f	4-Ethylphenyl	613	>10000
5g	Cyclohexyl	316	1340
5h	Isopropyl	382	2360
5i		5390	>10000
5j	Phenylethyl	420	1880
5k		202	3090
5l	2-Pyridinyl	393	2180
5m		281	>10000

[a]The biological assays are described in detail in the supplemental information. Each value is the average of at least two independent experiments.

Table 2. Compounds 6a-g and potencies on $Ca_v3.2$ and $Ca_v1.2$

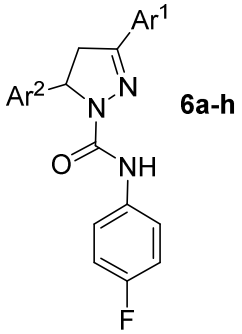

6a-h

Compound	Ar^1	Ar^2	$Ca_v3.2$ IC_{50} (nM)[a]	$Ca_v1.2$ IC_{50} (nM)[a]
6a	Phenyl	4-Fluorophenyl	25	>10000
6b	Methyl	4-Fluorophenyl	900	>10000
6c	4-Pyridinyl	4-Fluorophenyl	33	6400
(*R*)-6c	4-Pyridinyl	4-Fluorophenyl	320	7800
(*S*)-6c	4-Pyridinyl	4-Fluorophenyl	21	5400
6d	4-Pyridinyloxide	4-Fluorophenyl	110	>10000
6e	Phenyl	Methyl	410	3900
6f	Phenyl	4-Methylsulfonphenyl	40	>10000
6g	4-Pyridinyl	4-Methylsulfonphenyl	410	>10000

[a]The biological assays are described in details in the supplemental information. Each value is the average of at least two independent experiments.

Table 3. Compounds 11a-g and potencies on $Ca_v3.2$ and $Ca_v1.2$

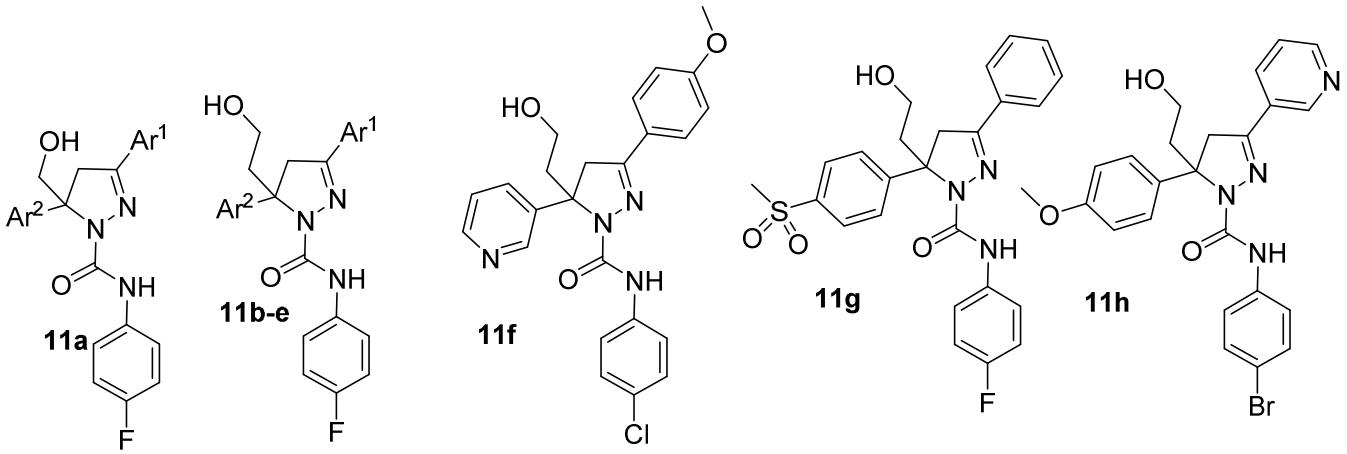

Compound	Ar^1	Ar^2	$Ca_v3.2$ IC_{50} (nM)[a]	$Ca_v1.2$ IC_{50} (nM)[a]
11a	Phenyl	4-Fluorophenyl	70	2650
11b	Phenyl	Phenyl	120	1940
11c	Phenyl	4-(Methoxyethoxy)phenyl	60	6300
11d	Phenyl	4-(Dimethylaminoethoxy)phenyl	>5300	>10000
11e	4-Pyridinyl	4-Toluyl	330	8600
11f	-	-	55	5700
11g	-	-	420	>10000
11h	-	-	140	>10000
(*R*)-11h	-	-	33	4800
(*S*)-11h	-	-	>10000	-

[a]The biological assays are described in details in the supplemental information. Each value is the average of at least two independent experiments.

Table 4. Compounds 11i-l and potencies on $Ca_v3.2$ and $Ca_v1.2$

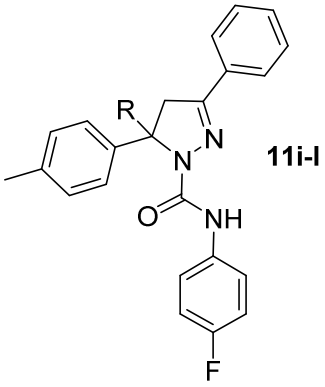

Compound	R	$Ca_v3.2$ IC_{50} (nM)[a]	$Ca_v1.2$ IC_{50} (nM)[a]
11i	Methoxymethyl	350	>10000
11j	Morpholinoethyl	430	5900
11k	Dimethylaminoethyl	240	2200
11l	1-(4-Methylpiperazinyl)ethyl	690	3600

[a]The biological assays are described in details in the supplemental information. Each value is the average of at least two independent experiments.

Table 5. Solubility profile of selected compounds

Compd	Aq. buffer pH4 (mg/L)	Aq. buffer pH7 (mg/L)	PSA ($Å^2$)	clogP	Compd	Aq. buffer pH4 (mg/L)	Aq. buffer pH7 (mg/L)	PSA ($Å^2$)	clogP
5b	<1	-	32	5.5	**11c**	8	8	83	4.5
5d	<1	<1	32	5.6	**11e**	193	35	78	4.0
5e	<1	<1	42	5.4	**11f**	27	14	87	3.6
6a	<1	<1	45	4.9	**11j**	371	1	57	5.2
6c	33	2	58	3.4	**11k**	42	30	48	5.2
6f	<1	<1	87	3.8	**11l**	477	158	51	5.3
11a	-	2	65	4.3					

Table 6. MDR1-assay on three compounds[a]

Compd.	P_{app} A→B (10^{-6} cm/s)	P_{app} B→A (10^{-6} cm/s)	Efflux ratio	PSA (Å^2)
6c	45	44	1.0	58
11f	5.3	90	17	87
11g	0.6	62	104	107

[a]Assay conditions: 1 μM compound concentration

Table 7. Characterization of compound 6c

Blockade of $Ca_v3.1$ in nM (FLIPR / QPatch -60 mV / QPatch -90 mV)[a]	29 / 450 / 1800
Blockade of $Ca_v3.2$ in nM (FLIPR / QPatch -60 mV / QPatch -90 mV)[a]	33 / 220 / 1700
Blockade of $Ca_v3.3$ in nM (FLIPR / QPatch -60 mV / QPatch -90 mV)[a]	340 / 2000 / 7000
Blockade of rat brain Na^+-channels at 10 μM in % (1^{st} peak / last peak)[a]	15 / 26
Blockade of rat brain K^+-channels at 10 μM in % (fast / slow)[a]	18 / 3
Inhibition of CYP3A4 in μM (with midazolam / testosterone as marker)	18 / 1.8
Inhibition of CYP2C9 in μM	1.8
Inhibition of CYP2D6 in μM	44
Microsomal metabolic stability in μL/min.mg protein (human / rat /mouse)	21 / 104 / 37
Unbound fraction (human plasma / rat plasma)	0.02 / 0.03

[a]See text and experimental part for details.

Table 8. Pharmacokinetic data for compound 6c

	iv				po			
Species / conditions	Dose (mg/kg)	Cl (mL/min·kg)	V_{ss} (L/kg)	$T_{1/2}$ (h)	Dose (mg/kg)	C_{max} (nM)	T_{max} (h)	F (%)
Wistar rats	0.2	110	23	7.1	2	27	0.25	4
Wistar rats + aminobenzotriazol	0.2	1.6	17	120	2	150	6.6	100
Beagle dogs					10	160	0.75	

Table 9. Plasma and brain concentrations in Wistar rats for compound 6c

Dose (mg/kg)	Collection time (h)	Plasma concentration (nM)	Brain concentration (nM)	CSF concentration (nM)
100	1	1230	4270	61
30	1	630	2570	47
10	1	270	800	19
10	3	290	1150	29

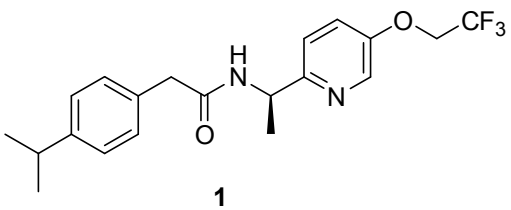

1

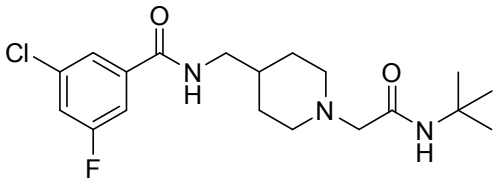

2

Figure 1. Selected TTCC blockers that have been in clinical development.

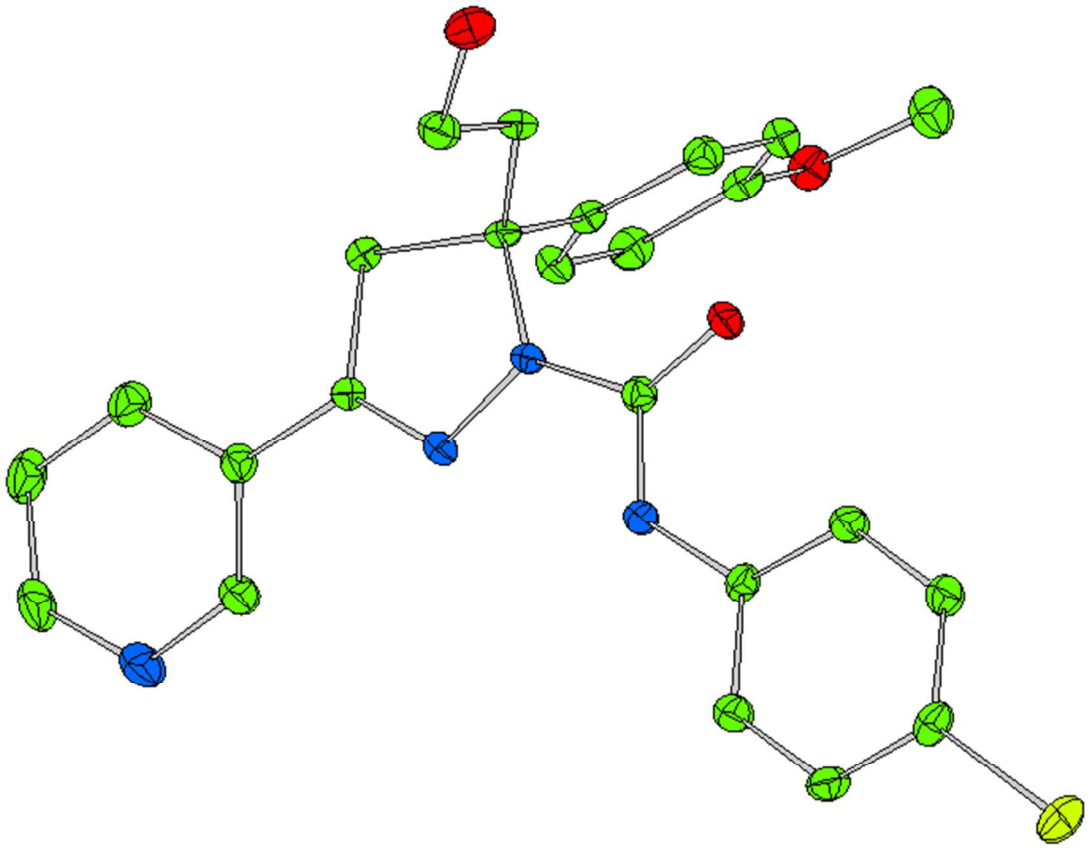

Figure 2. X-ray structure analysis of compound (*S*)-11h

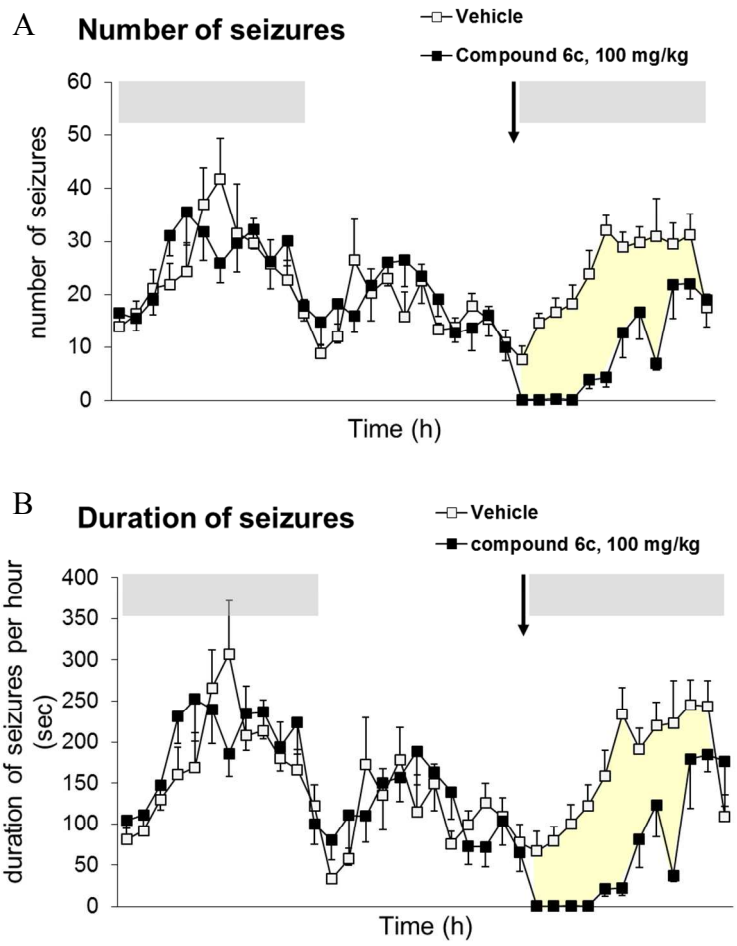

Figure 3: Effect of oral administration (arrow) of 100 mg/kg of compound 6c (■) or vehicle (□) on number (A) and duration (B) of spontaneous generalized, absence-type seizures per 1h intervals in WAG/Rij rats implanted with radiotelemetry for continuous EEG recording.

Data are represented as mean ± SEM over night (grey bar) and day periods (n = 7 per group).

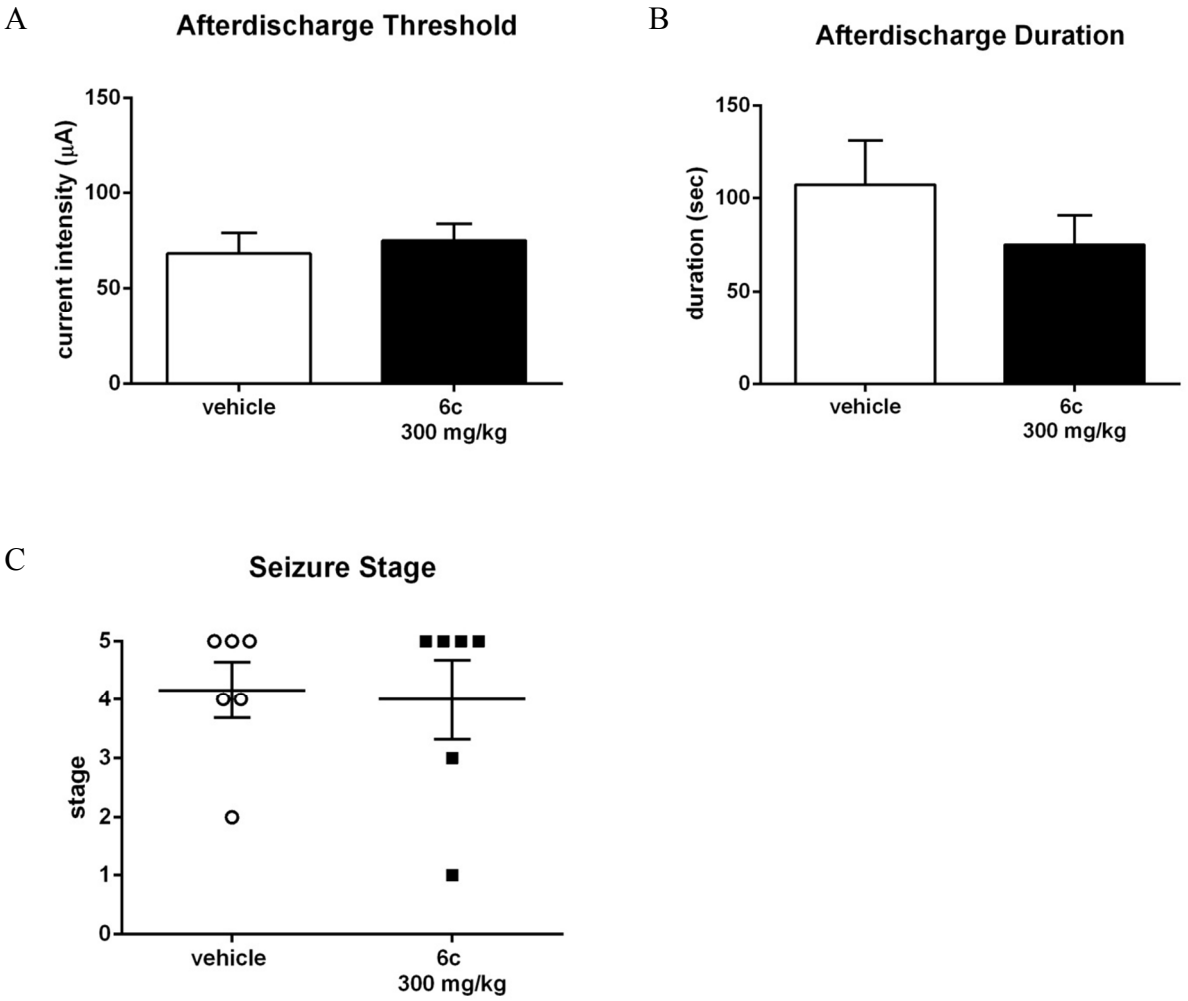

Figure 4: Effect of oral administration of 300 mg/kg of compound 6c (■) or vehicle (□) on afterdischarge threshold (A), afterdischarge duration (B) and seizure stage (C) in fully kindled rats, a model for temporal lobe epilepsies.

Compound or vehicle was given 2 h before stimulation and data are expressed as mean ± SEM (n = 6 per group).

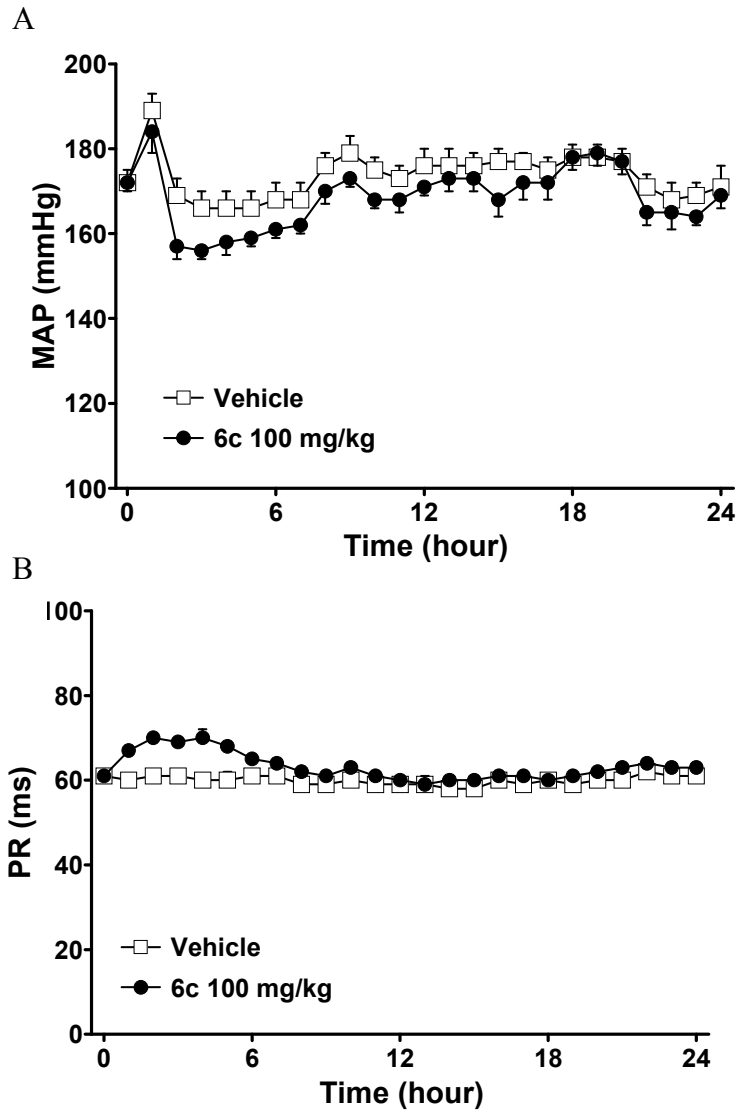

Figure 5: Effect of oral administration of 100 mg/kg of compound 6c (●) or vehicle (□) on mean arterial pressure (A) and PR-intervals (B) in conscious freely moving male spontaneous hypertensive rats.

Compound or vehicle was given at time 0 and data are represented as mean ± SEM (n = 8 per group).

Scheme 1. Preparation of dihydropyrazoles.[a]

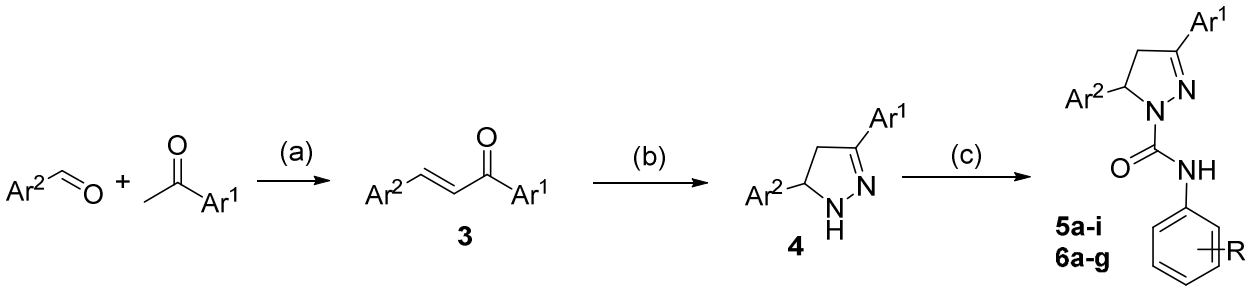

(a) KOH, EtOH, Et_2O, rt, 1 h (b) $H_2NNH_2 \cdot H_2O$, toluene, rt, 24 h. (c) Isocyanate, Et_3N, toluene, 90 °C, 1 h.

Scheme 2. Preparation of quaternized dihydropyrazoles.[a]

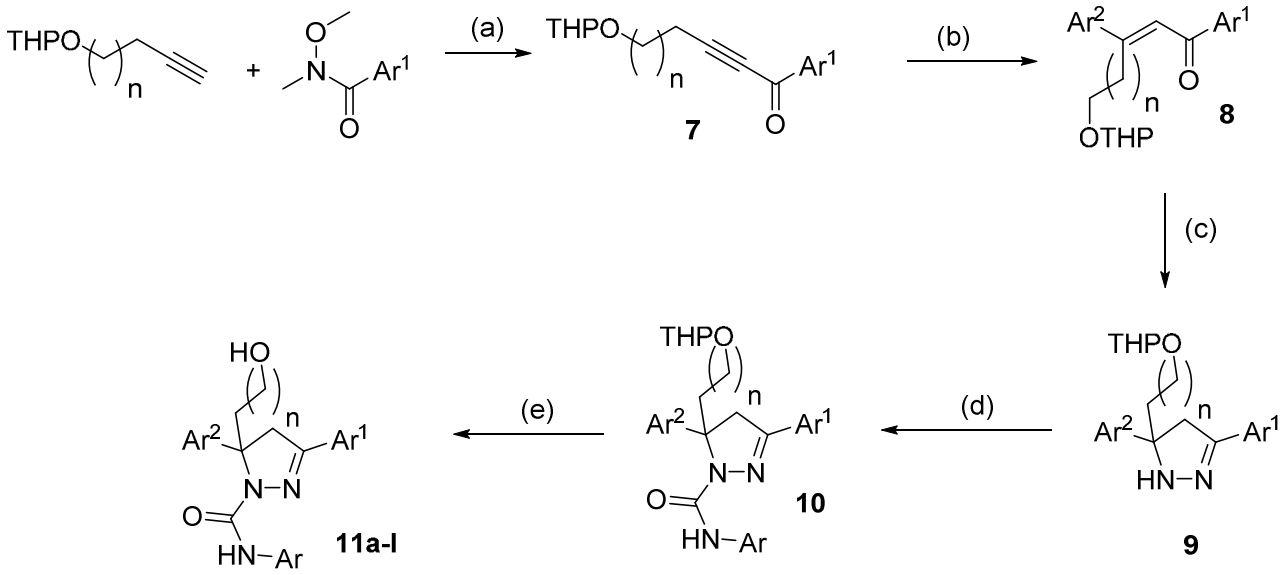

(a) BuLi, THF, -78 °C to rt, 2 h. (b) Ar^2MgBr, $CuBr \cdot Me_2S$. (c) $H_2NNH_2 \cdot H_2O$. (d) ArNCO. (e) PTSA.

TOC

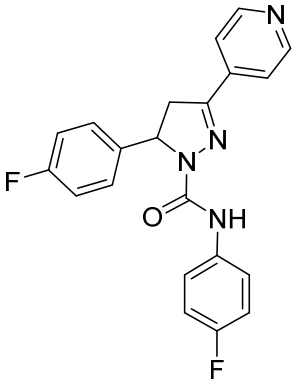

$Ca_V3.1$: IC_{50} = 29 nM
$Ca_V3.2$: IC_{50} = 33 nM
$Ca_V3.3$: IC_{50} = 340 nM

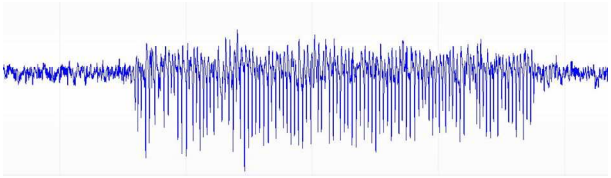

Absence seizure in wag/rij rats